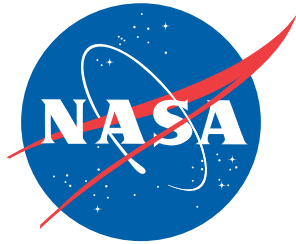


NASA/TM-2011-217072/Volume I  
NESC-RP-09-00506



# Space Shuttle Program (SSP) Orbiter Main Propulsion System (MPS) Gaseous Hydrogen ( $\text{GH}_2$ ) Flow Control Valve (FCV) Poppet Eddy Current (EC) Inspection Probability of Detection (POD) Study

*Robert S. Piascik/NESC and William H. Prosser/NESC  
Langley Research Center, Hampton, Virginia*

## NASA STI Program . . . in Profile

Since its founding, NASA has been dedicated to the advancement of aeronautics and space science. The NASA scientific and technical information (STI) program plays a key part in helping NASA maintain this important role.

The NASA STI program operates under the auspices of the Agency Chief Information Officer. It collects, organizes, provides for archiving, and disseminates NASA's STI. The NASA STI program provides access to the NASA Aeronautics and Space Database and its public interface, the NASA Technical Report Server, thus providing one of the largest collections of aeronautical and space science STI in the world. Results are published in both non-NASA channels and by NASA in the NASA STI Report Series, which includes the following report types:

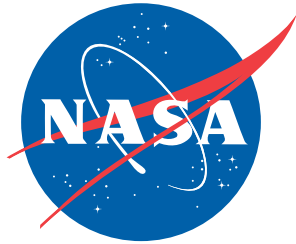
- TECHNICAL PUBLICATION. Reports of completed research or a major significant phase of research that present the results of NASA programs and include extensive data or theoretical analysis. Includes compilations of significant scientific and technical data and information deemed to be of continuing reference value. NASA counterpart of peer-reviewed formal professional papers, but having less stringent limitations on manuscript length and extent of graphic presentations.
- TECHNICAL MEMORANDUM. Scientific and technical findings that are preliminary or of specialized interest, e.g., quick release reports, working papers, and bibliographies that contain minimal annotation. Does not contain extensive analysis.
- CONTRACTOR REPORT. Scientific and technical findings by NASA-sponsored contractors and grantees.
- CONFERENCE PUBLICATION. Collected papers from scientific and technical conferences, symposia, seminars, or other meetings sponsored or co-sponsored by NASA.
- SPECIAL PUBLICATION. Scientific, technical, or historical information from NASA programs, projects, and missions, often concerned with subjects having substantial public interest.
- TECHNICAL TRANSLATION. English-language translations of foreign scientific and technical material pertinent to NASA's mission.

Specialized services also include creating custom thesauri, building customized databases, and organizing and publishing research results.

For more information about the NASA STI program, see the following:

- Access the NASA STI program home page at <http://www.sti.nasa.gov>
- E-mail your question via the Internet to [help@sti.nasa.gov](mailto:help@sti.nasa.gov)
- Fax your question to the NASA STI Help Desk at 443-757-5803
- Phone the NASA STI Help Desk at 443-757-5802
- Write to:  
NASA STI Help Desk  
NASA Center for AeroSpace Information  
7115 Standard Drive  
Hanover, MD 21076-1320

NASA/TM-2011-217072/Volume I  
NESC-RP-09-00506



# Space Shuttle Program (SSP) Orbiter Main Propulsion System (MPS) Gaseous Hydrogen ( $\text{GH}_2$ ) Flow Control Valve (FCV) Poppet Eddy Current (EC) Inspection Probability of Detection (POD) Study

*Robert S. Piascik/NESC and William H. Prosser/NESC  
Langley Research Center, Hampton, Virginia*

National Aeronautics and  
Space Administration


Langley Research Center  
Hampton, Virginia 23681-2199

March 2011

The use of trademarks or names of manufacturers in the report is for accurate reporting and does not constitute an official endorsement, either expressed or implied, of such products or manufacturers by the National Aeronautics and Space Administration.


Available from:

NASA Center for Aerospace Information  
7115 Standard Drive  
Hanover, MD 21076-1320  
443-757-5802

	<b>NASA Engineering and Safety Center Technical Assessment Report</b>	Document #: <b>NESC-RP- 09-00506</b>	Version: <b>1.1</b>
Title: <b>STS-126 MPS#2 GH<sub>2</sub> Flow Control Valve Broken Poppet</b>			Page #: 1 of 59

**Space Shuttle Program (SSP) Orbiter  
Main Propulsion System (MPS) Gaseous Hydrogen  
(GH<sub>2</sub>) Flow Control Valve (FCV) Poppet Eddy  
Current (EC) Inspection Probability of Detection  
(POD) Study**

**March 3, 2011**


	<b>NASA Engineering and Safety Center Technical Assessment Report</b>	Document #: <b>NESC-RP- 09-00506</b>	Version: <b>1.1</b>
		Title: <b>STS-126 MPS#2 GH<sub>2</sub> Flow Control Valve Broken Poppet</b>	

### Approval and Document Revision History

Note: NESC Director's signature is not required for this version.

Approved: _____	Original Signature on File	3/8/11
NESC	Director	Date

Version	Description of Revision	Office of Primary Responsibility	Effective Date
1.0	Initial Release	Dr. Robert S. Piascik, NASA Technical Fellow, Materials, LaRC	3/3/11
1.1	A figure number reference was bumped one number (pp 54 and 56)	Dr. Robert S. Piascik, NASA Technical Fellow, Materials, LaRC	3/11/11

	<b>NASA Engineering and Safety Center Technical Assessment Report</b>	Document #: <b>NESC-RP- 09-00506</b>	Version: <b>1.1</b>
		Title: <b>STS-126 MPS#2 GH<sub>2</sub> Flow Control Valve Broken Poppet</b>	

## Table of Contents

### Volume I: Technical Report

<b>1.0</b>	<b>Authorization and Notification</b> .....	<b>6</b>
<b>2.0</b>	<b>Signature Page</b> .....	<b>7</b>
<b>3.0</b>	<b>Team List</b> .....	<b>8</b>
<b>4.0</b>	<b>Executive Summary</b> .....	<b>9</b>
<b>5.0</b>	<b>Background</b> .....	<b>10</b>
5.1	Study Objective.....	11
5.2	Material.....	12
5.3	Poppet Simulator Test Procedure.....	13
5.3.1	Poppet Simulator Design.....	13
5.3.2	Test Fixtures and Fatigue Loading Procedure.....	14
5.3.3	Fatigue Crack Characterization Methods.....	18
5.3.3.1	Laboratory EC Inspection.....	18
5.3.3.2	SEM Examination.....	20
5.4	Crack Characterization Results.....	22
5.4.1	SEM Surface Analysis.....	23
5.4.2	Destructive Examination Results.....	27
5.5	EC Simulated Poppet POD Testing and Analysis.....	33
5.5.1	Hit/Miss Analysis.....	40
5.5.2	Signal Analysis.....	42
5.5.2.1	Longest Surface Crack Length as Explanatory Variable.....	44
5.5.2.2	Cumulative Surface Crack Length as Explanatory Variable.....	47
5.5.2.3	Cumulative Crack Area in Restricted Geography as Explanatory Variable.....	49
<b>6.0</b>	<b>Discussion of Summary Results</b> .....	<b>53</b>
<b>7.0</b>	<b>Findings and NESC Recommendations</b> .....	<b>55</b>
7.1	Findings.....	56
7.2	NESC Recommendations.....	56
<b>8.0</b>	<b>Alternate Viewpoints</b> .....	<b>57</b>
<b>9.0</b>	<b>Other Deliverables</b> .....	<b>57</b>
<b>10.0</b>	<b>Lessons Learned</b> .....	<b>57</b>
<b>11.0</b>	<b>Definition of Terms</b> .....	<b>57</b>
<b>12.0</b>	<b>Acronyms List</b> .....	<b>58</b>
<b>13.0</b>	<b>References</b> .....	<b>59</b>

### List of Figures

Figure 5.0-1.	Cracked STS-126 GH <sub>2</sub> FCV.....	11
Figure 5.3-1.	A Schematic of the Poppet Simulators and Extension Rods that were used in the NDE Study.....	13


	<b>NASA Engineering and Safety Center Technical Assessment Report</b>	Document #: <b>NESC-RP- 09-00506</b>	Version: <b>1.1</b>
Title: <b>STS-126 MPS#2 GH<sub>2</sub> Flow Control Valve Broken Poppet</b>		Page #: 4 of 59	

Figure 5.3-2.	Poppet Simulator and Loading Fixture .....	14
Figure 5.3-3.	Image of Poppet Simulator Loaded in a Test Fixture .....	15
Figure 5.3-4.	The Number of Cycles required to Initiate Fatigue Cracks as a Function of the maximum Compressive Load .....	16
Figure 5.3-5.	Test Fixture with Displacement Gage for Detecting Cracking using the Compliance Method .....	17
Figure 5.3-6.	Example of a Compliance Curve used to Detect Crack Growth in a Poppet Simulator Test .....	18
Figure 5.3-7.	Image of the EC System used to Screen the Poppet Simulators for Cracks .....	19
Figure 5.3-8.	EC Scan Result for a Poppet Simulator with Two Distinct Fatigue Cracks .....	20
Figure 5.3-9.	Illustration of the High Stress Regions of the Poppet Simulators that were examined during the SEM Inspections.....	21
Figure 5.3-10.	SEM Images of a Crack in a Poppet Simulator with Repliset and after the Repliset has Been Removed.....	21
Figure 5.3-11.	Example of the Fracture Surface Morphology that Resulted from the Marking Process ..	22
Figure 5.4-1.	Example of an SEM Image that shows the Location of Two Cracks .....	24
Figure 5.4-2.	Example of an SEM image that shows Sufficient Details to Measure the Lengths and Relative Positions of Two Cracks.....	25
Figure 5.4-3.	Distribution of the Largest Crack per Loaded Region of the Poppet Simulators Tested..	25
Figure 5.4-4.	Image of a Poppet Crack at 10,000x Magnification with Crack Openings Measured at Several Locations.....	26
Figure 5.4-5.	Crack Opening Displacement for Several Poppets.....	27
Figure 5.4-6.	Images of a Fracture Surface from a Poppet Simulator and the Cracks observed on the Surface prior to Destructive Examination.....	29
Figure 5.4-7.	Comparison of the Surface Crack Length Measured and after Destructive Examination of Crack #4 from Figure 5.4-6 .....	30
Figure 5.4-8.	Comparison of the Surface Crack Length Measured and after Destructive Examination of Crack #6 from Figure 5.4-6 .....	<b>Error! Bookmark not defined.</b>
Figure 5.4-9.	Aspect Ratio of several Cracks from Poppet Simulators and Flight Poppets obtained from the Destructive Examinations .....	32
Figure 5.4-10.	Image of the Crack Detected in Flight Poppet from STS-126.....	33
Figure 5.4-11.	Measured Crack Depth from the Destructive Examinations as a Function of the Surface Crack Length.....	33
Figure 5.5-1.	US 1779 (UniWest) Bolt Inspection Scanner .....	34
Figure 5.5-2.	US 454 (UniWest) EC Crack Detector .....	35
Figure 5.5-3.	EC Bolt Thread Root Inspection Probe US 1839 .....	35
Figure 5.5-4.	S/N 33 Poppet Standard.....	36
Figure 5.5-5.	EC Voltage Scan of S/N 33-361 Standard.....	37
Figure 5.5-6.	EC Phase Diagram of S/N 33-361 Standard.....	37
Figure 5.5-7.	Estimated POD Curves from Hit/Miss Data. 95 Percent Confidence on Crack Size yielding a Probability of Detection of 0.90 is shown for Inspector 1 .....	41
Figure 5.5-8.	The Vpp Response of Inspector 2 versus Inspector 1 .....	42
Figure 5.5-9.	Standard Deviation versus Mean of the Vpp Responses (combined for both inspectors) for Individual poppet Simulator Inspections.....	43
Figure 5.5-10.	Standard Deviation versus Mean of the Vpp Responses Transformed by a Power of 0.6 (combined for both inspectors) for Individual Poppet Simulator Inspections .....	44




	<b>NASA Engineering and Safety Center Technical Assessment Report</b>	Document #: <b>NESC-RP- 09-00506</b>	Version: <b>1.1</b>
Title: <b>STS-126 MPS#2 GH<sub>2</sub> Flow Control Valve Broken Poppet</b>		Page #: 5 of 59	


Figure 5.5-11.	Transformed Response versus Largest Crack Length for Individual Poppet Simulator Inspections .....	45
Figure 5.5-12.	Linear Fit in the Transform Scale with Censored Data Shown .....	46
Figure 5.5-13.	Estimated POD Curves from Signal Strength ( $V_{pp}$ ) versus size of Longest Crack. The 95 percent confidence on Crack Length Yielding a Probability of Detection of 0.90 is shown for Threshold Level. ....	47
Figure 5.5-14.	Transformed Response versus Cumulative Crack Lengths .....	48
Figure 5.5-15.	Estimated POD curves from signal strength ( $V_{pp}$ ) versus sum of all Crack Lengths in loaded region. The 95 percent confidence on crack length yielding a probability of detection of 0.90 is shown for threshold level. ....	49
Figure 5.5-16.	Illustration of the Use of a 0.040 inch (1.0 mm) Circle for Accumulating Crack Area....	50
Figure 5.5-17.	Transformed signal versus maximum cumulative area within 0.04 inch (1.0 mm) circle. Regions containing single cracks larger than 0.040 inch (1.0 mm) are shown with cross sectional area from the largest single crack. ....	51
Figure 5.5-18.	Transformed signal versus maximum cumulative area within 0.04 inch (1.0 mm) circle. Regions containing single cracks larger than 0.040 inch (1.0 mm) are shown with cross sectional area from the largest single crack. ....	52
Figure 5.5-19.	Estimated POD curves from signal strength ( $V_{pp}$ ) versus Cumulative Cross-Sectional area of Flaws within 0.04 inch (1.0 mm) circle .....	53
Figure 6.0-1.	Estimated POD curves of Figure 5.5-19 with the x-axis transformed to the single surface crack length yielding the cross-sectional area estimates.....	54

### List of Tables

Table 5.2-1	Heat Treatment Schedule for the 440A Stainless Steel .....	12
Table 5.4-1.	Summary of the Number of Cracks Found in Each Poppet.....	26
Table 5.4-2.	Summary of the Crack Depth Measurements from the Poppet Simulator Specimens that were Destructively Examined.....	32
Table 5.5-1.	Summary of SEM Characterization and Inspection Findings.....	39
Table 5.5-2.	Number of Loaded Regions with Known Cracks and the Reported Responses .....	40
Table 5.5-3.	Inspection Findings Based on the Largest Crack Length in a Loading Region.....	40
Table 6.0-1.	Summary of $\alpha_{90}$ Estimates and Uncertainty. ....	55

## Volume II: Appendices (stand-alone volume)

- A. Poppet Specimen Data
- B. Boeing Eddy Current Procedure/Technique Sheet Flow Control Valve Poppet - #SSO-01  
Revision C


	<b>NASA Engineering and Safety Center Technical Assessment Report</b>	Document #: <b>NESC-RP- 09-00506</b>	Version: <b>1.1</b>
Title: <b>STS-126 MPS#2 GH<sub>2</sub> Flow Control Valve Broken Poppet</b>		Page #: 6 of 59	

## **Volume I: Technical Report**

### **1.0 Authorization and Notification**

Mr. Ralph Roe, the Director of the NASA Engineering and Safety Center (NESC), requested an independent assessment of the anomalous gaseous hydrogen (GH<sub>2</sub>) flow incident on the Space Shuttle Program (SSP) Orbiter Vehicle (OV)-105 during the Space Transportation System (STS)-126 mission. The main propulsion system (MPS) engine #2 GH<sub>2</sub> flow control valve (FCV) LV-57 transition from low towards high flow position without being commanded. Post-flight examination revealed that the FCV LV-57 poppet had experienced a fatigue failure that liberated a section of the poppet flange. The NESC assessment provided a peer review of the computational fluid dynamics (CFD), stress analysis, and impact testing. A probability of detection (POD) study was requested by the SSP Orbiter Project for the eddy current (EC) nondestructive evaluation (NDE) techniques that were developed to inspect the flight FCV poppets.

An out-of-board activity was approved February 5, 2009. The final report was presented to the NESC Review Board (NRB) for approval on March 3, 2011.

	<b>NASA Engineering and Safety Center Technical Assessment Report</b>	Document #: <b>NESC-RP- 09-00506</b>	Version: <b>1.1</b>
Title: <b>STS-126 MPS#2 GH<sub>2</sub> Flow Control Valve Broken Poppet</b>		Page #: 7 of 59	

## 2.0 Signature Page

### Assessment Team Members

Submitted by:

*Team Signature Page on File – 3-14-11*

\_\_\_\_\_

Dr. Robert S. Piascik

\_\_\_\_\_

Date

\_\_\_\_\_

Dr. William H. Prosser

\_\_\_\_\_


Date

Significant Contributors:

\_\_\_\_\_


Dr. David S. Dawicke Date

Signatories declare the findings and observations compiled in the report are factually based from data extracted from Program/Project documents, contractor reports, and open literature, and/or generated from independently conducted tests, analysis, and inspections.

	<b>NASA Engineering and Safety Center Technical Assessment Report</b>	Document #: <b>NESC-RP- 09-00506</b>	Version: <b>1.1</b>
		Title: <b>STS-126 MPS#2 GH<sub>2</sub> Flow Control Valve Broken Poppet</b>	

### 3.0 Team List

Name	Discipline	Organization/Location
<b>Core Team</b>		
Dr. Robert Piascik	NASA Technical Fellow, Materials LaRC	
Dr. William Prosser	NASA Technical Fellow, NDE	LaRC
David Dawicke	Fracture Mechanics	AS&M
John “Andy” Newman	Materials Engineer	LaRC
Floyd Spencer	NDE	Sandia National Laboratories
Ajay Koshti	Materials Engineer	JSC
Rick Russell	Materials Engineer	KSC
Harold “Clay” Claytor	Materials Technician	Lockheed Martin Corporation
William Johnston	Materials Engineer	Lockheed Martin Corporation
James Baughman	SEM Technician	Lockheed Martin Corporation
Scott Willard	Materials Engineer	Lockheed Martin Corporation
Russell “Buzz” Wincheski NDE		LaRC
Diana Kerns	MTSO Program Analyst	LaRC
<b>Consultants</b>		
Bud Castner	Metals	JSC
Robert DeVries	NDE Boeing	Company
James Engle	NDE	Boeing Company
<b>Support</b>		
Terri Derby	Project Coordinator	LaRC, ATK
Erin Moran	Technical Writer	LaRC, ATK


	<b>NASA Engineering and Safety Center Technical Assessment Report</b>	Document #: <b>NESC-RP- 09-00506</b>	Version: <b>1.1</b>
Title: <b>STS-126 MPS#2 GH<sub>2</sub> Flow Control Valve Broken Poppet</b>		Page #: 9 of 59	

## 4.0 Executive Summary

Space Shuttle Program (SSP) Orbiter Vehicle (OV)-105, *Endeavour*, as part of the Space Transportation System (STS)-126, experienced an in-flight fatigue failure of one of the three Space Shuttle Main Engine (SSME) gaseous hydrogen (GH<sub>2</sub>) flow control valve (FCV) poppets. This type of failure has a remote potential consequence of the loss of the vehicle, so a root cause investigation was undertaken and the remaining FCV poppets were subjected to rigorous inspections. Newly developed eddy current (EC) nondestructive evaluation (NDE) methods were successfully used to detect cracks, but probability of detection (POD) evaluations of the NDE methods had not been performed. The lack of a POD evaluation results in an uncertainty of the sensitivity and accuracy of EC NDE methods being used to inspect flight FCV poppets.

A POD evaluation was conducted for the EC system currently being used to inspect flight poppets using cracked poppet simulators. The poppet simulator was designed to replicate the relevant physical features of the flight FCV poppets including: flight approved material and heat treatment schedule, poppet dimensions, and naturally occurring fatigue cracks that nucleated in the same location, shape, and size as those found in STS-126 and other flight FCV poppets. The fatigue cracks were nucleated in the poppet simulators by using a specially designed fixture that mechanically loaded the critical poppet location. Each cracked poppet simulator was examined using EC NDE and a scanning electron microscope (SEM) to identify the size and location of each crack greater than 0.001 inches (0.03 mm).

A total of 55 cracked poppet simulators were created for the POD study. These poppet simulators had a distribution of cracks with lengths from 0.001 to more than 0.1 inches (0.025 to more than 2.54 mm). The measurements for the POD study were performed by two independent and certified inspectors with identical EC systems, and both inspectors conducted six examinations of each cracked poppet simulator. In the absence of a specific allowable critical crack size from structural analysis, the flight poppet inspection from the EC system currently being used should continue to reject on any signals greater than the 0.2 volt threshold.

	<b>NASA Engineering and Safety Center Technical Assessment Report</b>	Document #: <b>NESC-RP- 09-00506</b>	Version: <b>1.1</b>
Title: <b>STS-126 MPS#2 GH<sub>2</sub> Flow Control Valve Broken Poppet</b>		Page #: 10 of 59	


## 5.0 Background

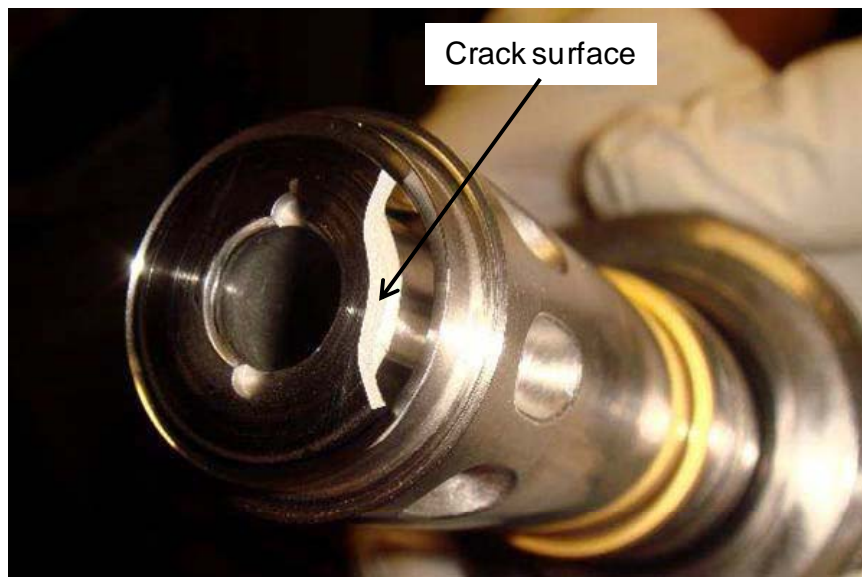
OV-105 experienced an in-flight (STS-126) fatigue failure of one of the three SSME FCV poppets. This type of failure has a remote potential consequence of the loss of the vehicle, so a root cause investigation was undertaken and the remaining FCV poppets were subjected to rigorous inspections. Newly developed EC NDE methods were successfully used to detect cracks, but POD evaluations of the NDE methods had not been performed. This report describes a study that conducted a POD analysis to develop a quantifiable understanding of the size of FCV poppet cracks that can be found, and conversely missed, by an inspection.

Each SSME has a FCV that adjusts the flow of GH<sub>2</sub> to the External Tank (ET), which regulates the tank pressure during SSME operation. The GH<sub>2</sub> flow through the FCVs is restricted by a poppet valve that has two flow positions (high and low), and the FCVs from the three SSMEs are controlled independently to maintain the proper ET pressure as the liquid hydrogen (LH<sub>2</sub>) fuel is consumed. The ET pressurization system is designed to successfully operate with only two of the three FCVs. An ET vent valve will actuate to relieve the pressure when the ET internal pressure exceeds 35 pounds per square inch (psi). The failure of a FCV presents two concerns:

1. The venting of GH<sub>2</sub> presents an ignition risk for the early portion of the ascent.
2. The liberation of a portion of the FCV could rupture downstream pressure lines, exasperating the venting problem and potentially causing an over pressurization in the Orbiter aft section.

Flight controllers identified that GH<sub>2</sub> was flowing from one FCV at a higher than commanded rate during the STS-126 mission in November 2008. The flow rates in the other two FCVs were automatically reduced and no unusual ET pressurization issues were observed during ascent. The MPS was inspected after landing and the FCV poppet was observed to have a segment missing, as shown in Figure 5.0-1. The damaged FCV was removed from OV-105, disassembled, and fractographic examination determined that the crack was caused by fatigue.

	<b>NASA Engineering and Safety Center Technical Assessment Report</b>	Document #: <b>NESC-RP- 09-00506</b>	Version: <b>1.1</b>
Title: <b>STS-126 MPS#2 GH<sub>2</sub> Flow Control Valve Broken Poppet</b>		Page #: 11 of 59	



*Figure 5.0-1. Cracked STS-126 GH<sub>2</sub> FCV*

The subsequent STS-119 Flight Readiness Review determined that more information was needed on the FCV poppet cracking issue before proceeding to launch. A root cause analysis was initiated and the FCVs from all three Orbiters and flight spares were subjected to a rigorous inspection. The risk imposed to the Orbiter in the event of another poppet valve failure where a piece of the valve may be released into the GH<sub>2</sub> flow was also investigated.


The remaining flight and spare FCV poppets were examined using SEM inspection of the poppet fillet region, magnetic particle, and EC NDE. All three methods were successful, and locating cracks with SEM was initially considered as providing the most accurate identification of crack size and location, with EC inspection as being the most promising for field applications. However, a POD study has not been conducted for any of the three techniques.

## 5.1 Study Objective

The objective of this study was to conduct a POD study to characterize the behavior of a newly developed EC NDE method used to find fatigue cracks in FCV poppets. The study consists of two efforts:

- Task 1: Create and fully characterize a statistically significant number of fatigue cracks in FCV poppet simulators that replicate in size, shape, and location the defects observed in the flight poppets.
- Task 2: Conduct a POD analysis for the EC NDE method using the cracked poppet simulators developed in Task 1.

The creation of cracked poppet simulators required the development of a specialized test procedure for initiating a distribution of small cracks (0.001 to greater than 0.10 inches, 0.025 to

	<b>NASA Engineering and Safety Center Technical Assessment Report</b>	Document #: <b>NESC-RP- 09-00506</b>	Version: <b>1.1</b>
Title: <b>STS-126 MPS#2 GH<sub>2</sub> Flow Control Valve Broken Poppet</b>		Page #: 12 of 59	

more than 2.54 mm) in the fillet of the poppet simulators. Each cracked poppet simulator was examined using a SEM to characterize the number, size, and location of all surface cracks. The SEM findings were assumed to have identified all cracks greater than 0.001 inches (0.03 mm) in surface length and were the standards that were used to evaluate the EC NDE method. A portion of the cracked poppet simulators were destructively examined to validate the surface SEM measurements and to characterize the crack shape, depth, and trajectory. The remaining poppet simulators were examined by two independent and certified NDE inspectors, and analyses of the results were used to establish a POD for locating cracks in the flight hardware. A catalog of all of the identified cracks was compiled to document the number of cracks, crack sizes, and crack locations for each poppet simulator.


## 5.2 Material

The GH<sub>2</sub> FCVs were made of 440A stainless steel. Flight-approved round bar stock of 440A steel material with a diameter of 0.75 inch (19 mm) was obtained from the Kennedy Space Center in the fully annealed state. The machined poppet simulators were heat-treated to attain a Rockwell C hardness (H<sub>RC</sub>) value of 54-58 to replicate the condition of the flight poppets. The heat treatment schedule, with a tolerance on all temperatures of ± 10°F (5.6°C), used in this study is provided in Table 5.2-1.

**Table 5.2-1. Heat Treatment Schedule for the 440A Stainless Steel**

Step	Activity
1	Clean parts with methanol.
2	Vacuum furnace: <ol style="list-style-type: none"> <li>Pump down to 10<sup>-6</sup> Torr.</li> <li>Heat at 2000°F (1093°C) per hour to 1900°F (1038°C), while at or below 10<sup>-4</sup> Torr.</li> <li>Hold part at temperature for 1 hour.</li> <li>Backfill with helium gas until part is below 225°F (107°C).</li> <li>Remove part.</li> </ol>
3	Within 30 minutes of removal from vacuum furnace, place parts in cold box at -120°F (-84°C). Hold at temperature for 2 hours
4	Remove parts from cold box and allow warming to ambient temperature.
5	Place parts in air furnace at 350°F (177°C); hold at temperature for 2 hours.
6	Remove parts from air furnace and allow cooling to ambient temperature
7	Place parts in cold box at -120°F (-84°C); Hold at temperature for 2 hours
8	Remove parts from cold box and allow warming to ambient temperature
9	Place parts in air furnace at 350°F (177°C); hold at temperature for 1 hour
10	Remove parts from air furnace and allow cooling to ambient temperature
11	Place parts in cold box at -120°F (-84°C); Hold at temperature for 1 hour
12	Remove parts from cold box and allow warming to ambient temperature
13	Perform hardness test to verify 54-58 H <sub>RC</sub>



	<b>NASA Engineering and Safety Center Technical Assessment Report</b>	Document #: <b>NESC-RP- 09-00506</b>	Version: <b>1.1</b>
Title: <b>STS-126 MPS#2 GH<sub>2</sub> Flow Control Valve Broken Poppet</b>		Page #: 13 of 59	

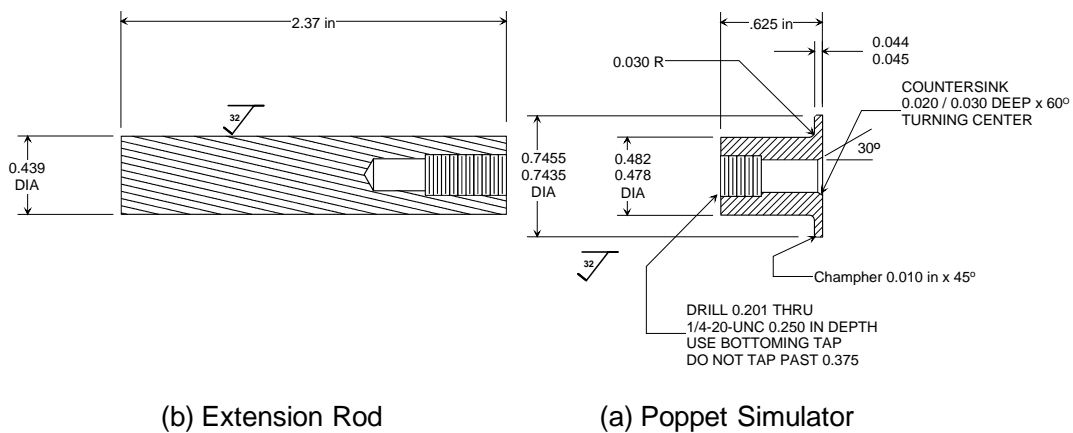
### 5.3 Poppet Simulator Test Procedure

Fatigue tests were conducted on poppet simulators to produce a distribution of cracks for a POD study of EC inspection methods. The poppet simulators were made of the same material and with the same critical dimensions of as the flight poppets to make inspection of the simulators as similar as possible to inspections of flight hardware. The following sections describe the design of the poppet simulators and testing procedures.


#### 5.3.1 Poppet Simulator Design

The poppet simulators were designed to have the same critical shaft, flange fillet radius, and flange thickness dimensions as the flight poppets. The diameter of the flange was about 0.12 inches (3 mm) larger than the flight poppet to provide sufficient surface area for the application of the cyclic test load. The length of the poppet and the details away from the flange radius were not relative to the POD study and were eliminated in the simulator design, as shown in Figure 5.3-1a. An extension rod was machined to facilitate the handling of the poppet simulators during inspection, as shown in Figure 5.3-1b. The end of the poppet simulator away from the flange was threaded for the attachment of the extension rod. The resulting poppet simulator was significantly shorter than the flight poppets, allowing the maximum number of poppet simulators to be machined from the limited supply of material.

The flange fillet radius of each poppet simulator was polished after machining to enhance crack detection. The poppet was rotated at about 90 revolutions per minute (rpm) and a diamond paste polishing grit was applied to the end of a sharpened wooden stick that was wrapped with a piece of cotton. Five different levels of polishing grit were used (9, 6, 3, 1, and ¼ micron) for 3 minutes each. An optical inspection was performed to verify that no remnant machining marks or scratches were present on the poppet simulator flange fillet radius which could have influenced the NDE inspections.

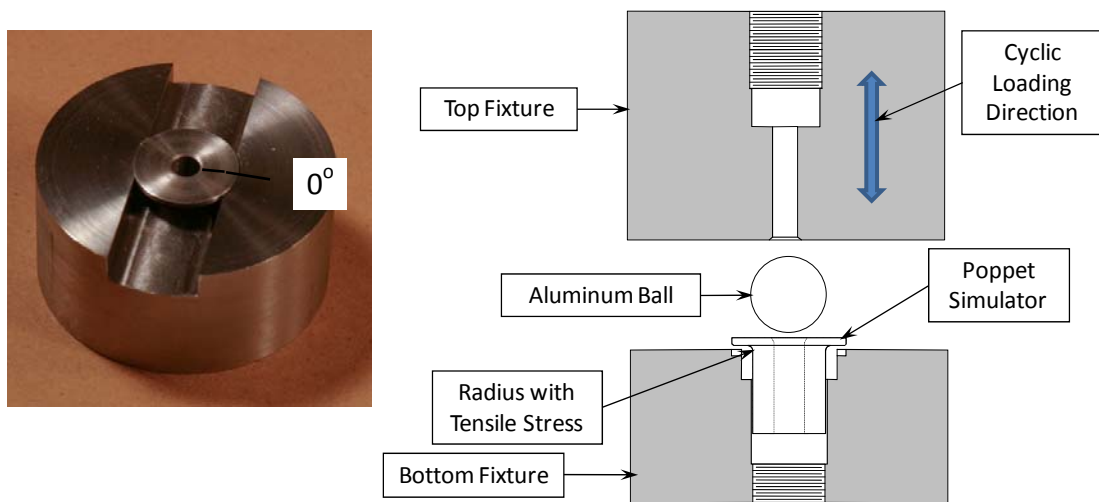


**Figure 5.3-1. A Schematic of the Poppet Simulators and Extension Rods that were used in the NDE Study**

	<b>NASA Engineering and Safety Center Technical Assessment Report</b>	Document #: <b>NESC-RP- 09-00506</b>	Version: <b>1.1</b>
Title: <b>STS-126 MPS#2 GH<sub>2</sub> Flow Control Valve Broken Poppet</b>		Page #: 14 of 59	

### 5.3.2 Test Fixtures and Fatigue Loading Procedure

The poppet simulator loading fixtures were designed to generate a tensile stress in a limited portion of the flange fillet radius, as shown in Figure 5.3-2. The bottom fixture supported the edge of the poppet simulator flange at two locations that were 180 degrees apart. The bottom of an aluminum ball rested on the hole in the center of the poppet simulator, and the top fixture applied a cyclic downward force to the top of the ball. The force from the ball was reacted by the two regions of the poppet simulator flange that were in contact with the bottom fixture. The highest tensile stress was in the flange fillet radius of the poppet simulator in the vicinity of the two loading regions. This reduced the required inspection region to about  $\pm 15$  degrees around the center of the two loading regions. A reference line was placed on the bottom fixture and on each poppet simulator to ensure consistent alignment when the simulators were removed for inspection. The subsequent inspection areas were referenced as the 0 or the 180 degree side. The reference line was removed after the SEM inspection and a new reference mark was etched into the edge of the flange at a random location relative to the 0 degree side to prevent the NDE inspectors from deducing the crack locations.




(b) Photograph of Bottom Fixture

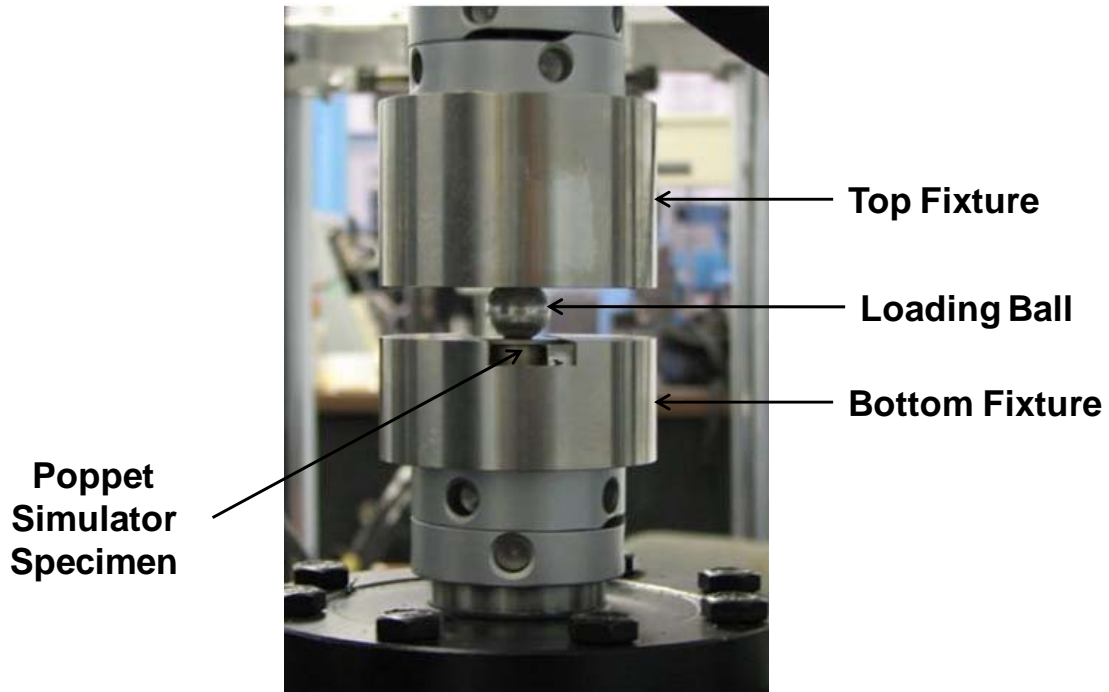
(a) Schematic of Loading Fixtures

**Figure 5.3-2. Poppet Simulator and Loading Fixture**


The fixtures were mounted to a servo-hydraulic load frame, as shown in Figure 5.3-3, and cycled under constant load at a stress ratio (minimum stress/maximum stress) of  $R = 0.1$  and frequencies of 35 to 65 Hz. A series of preliminary tests were conducted to determine the optimal maximum compressive load for initiating cracks and values between 350 and 500 pounds were found to be successful. Tests that were conducted above this level had small critical crack lengths and required few cycles to propagate a detectable crack to the critical crack size, making it nearly impossible to stop a test with a detectable crack. Tests that were conducted below this range required millions of cycles to initiate cracks. An empirical relationship between maximum

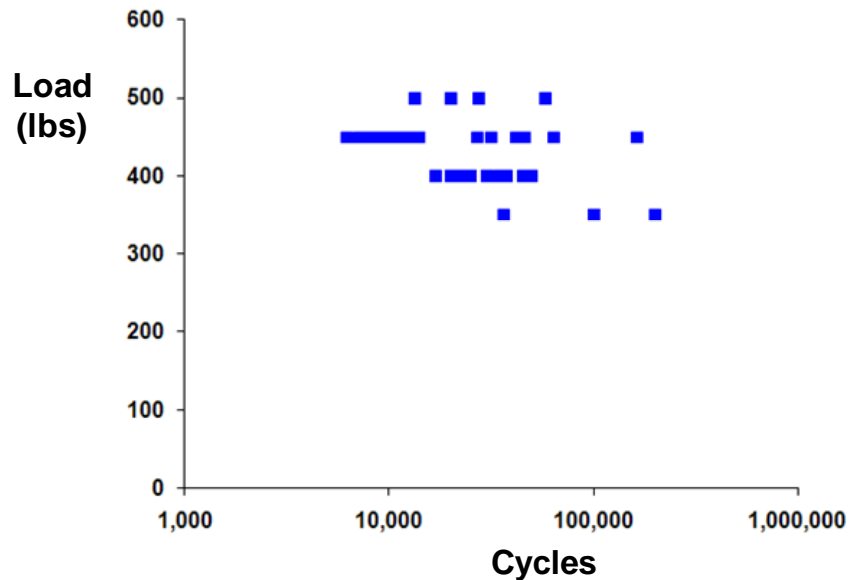
	<b>NASA Engineering and Safety Center Technical Assessment Report</b>	Document #: <b>NESC-RP-09-00506</b>	Version: <b>1.1</b>
Title: <b>STS-126 MPS#2 GH<sub>2</sub> Flow Control Valve Broken Poppet</b>		Page #: 15 of 59	

compressive load and the number of cycles required to initiate a fatigue crack is shown in Figure 5.3-4.



*Figure 5.3-3. Image of Poppet Simulator Loaded in a Test Fixture*


	<b>NASA Engineering and Safety Center Technical Assessment Report</b>	Document #: <b>NESC-RP-09-00506</b>	Version: <b>1.1</b>
Title: <b>STS-126 MPS#2 GH<sub>2</sub> Flow Control Valve Broken Poppet</b>		Page #: 16 of 59	



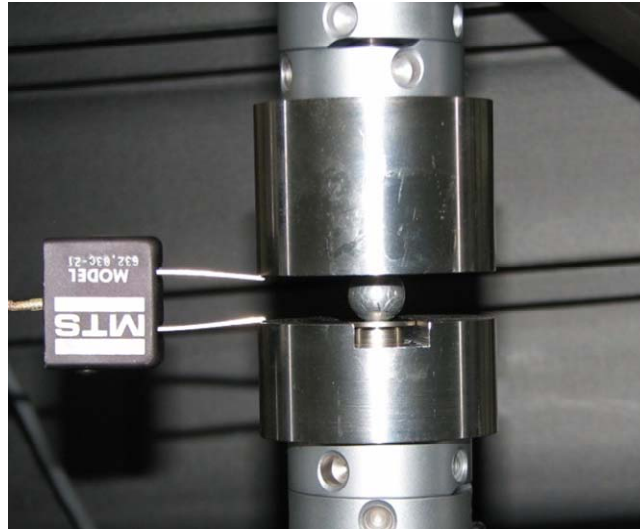
*Figure 5.3-4. The Number of Cycles required to Initiate Fatigue Cracks as a Function of the maximum Compressive Load*

Two methods were developed to stop the tests with sub-critical detectable cracks. The first, or manual method, determined a target number of cycles from sacrificial tests that were fatigue cycled until failure. Each poppet simulator was examined with an EC system prior to the fatigue cycling to establish a baseline response. The simulators were then fatigue cycled for a fraction of the target number of cycles, and then the poppet simulators removed and re-examined with an EC system. The poppet simulators were examined with an SEM to verify the presence of cracks only if a change in the baseline EC response was detected. The simulator loading continued for a small number of additional cycles if no cracks were located using the SEM. This technique successfully produced very small cracks (surface length ~0.001 inches (0.03 mm)), but also had many false calls and had cracks that grew to critical during the fatigue cycling between SEM/EC inspections.


The second, or automated, method of generating cracks used the calculated compliance (slope of the load – displacement curve) from the fixture displacements. The cyclic fatigue loading was stopped when a change in the compliance was observed. A displacement gage was placed between the top and bottom fixture, as shown in Figure 5.3-5. The compliance method acquired load and displacement data every 100 cycles, and then calculated the slope of the load versus fixture displacement data. An increase in the slope would indicate the possibility of a crack growing in the poppet simulator, reducing the stiffness of the flanges. The slope, or compliance, was plotted as a function of the number of applied cycles, as shown in Figure 5.3-6. Initially the compliance decreased with loading cycles as the aluminum ball seated in the hole of the poppet simulator. Eventually the influence of the aluminum ball seating was offset by the increasing

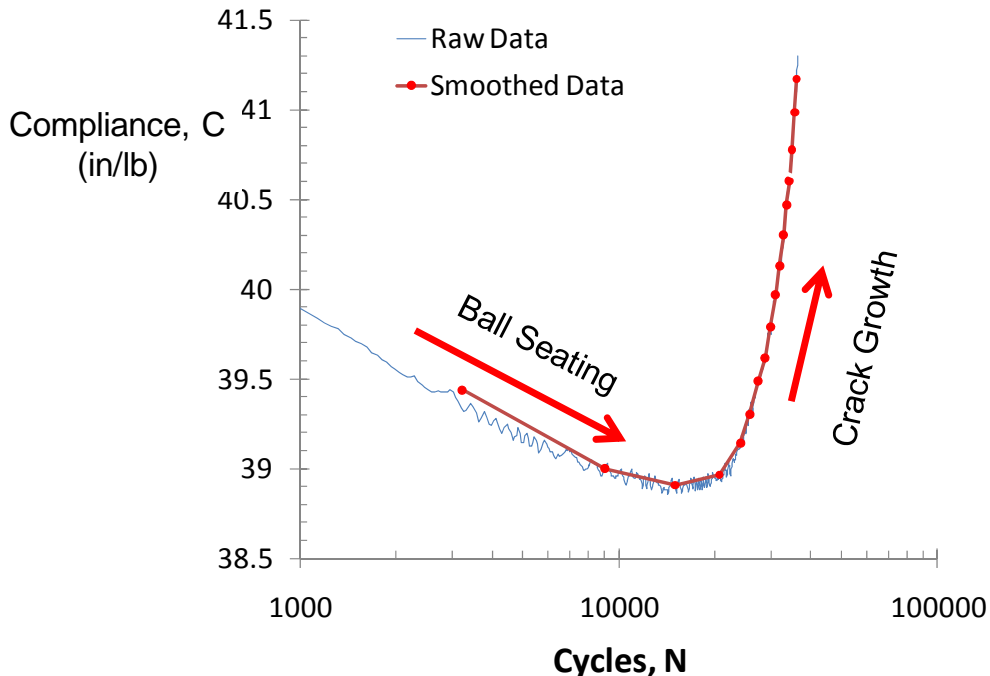
	<p align="center"><b>NASA Engineering and Safety Center Technical Assessment Report</b></p>	<p>Document #: <b>NESC-RP- 09-00506</b></p>	<p>Version: <b>1.1</b></p>
<p>Title: <b>STS-126 MPS#2 GH<sub>2</sub> Flow Control Valve Broken Poppet</b></p>		<p>Page #: 17 of 59</p>	

compliance of growing cracks and a rapid increase in overall compliance was observed. The resulting crack length in the poppet simulator could be adjusted, somewhat successfully, by stopping the tests at different magnitudes of compliance change. The poppet simulators were examined by SEM after each compliance cutoff and always had a crack with a surface length between 0.012 and 0.05 inches (0.3 to 1.3 mm).



*Figure 5.3-5. Test Fixture with Displacement Gage for Detecting Cracking using the Compliance Method*

	<b>NASA Engineering and Safety Center Technical Assessment Report</b>	Document #: <b>NESC-RP-09-00506</b>	Version: <b>1.1</b>
Title: <b>STS-126 MPS#2 GH<sub>2</sub> Flow Control Valve Broken Poppet</b>		Page #: 18 of 59	




*Figure 5.3-6. Example of a Compliance Curve used to Detect Crack Growth in a Poppet Simulator Test*

### 5.3.3 Fatigue Crack Characterization Methods

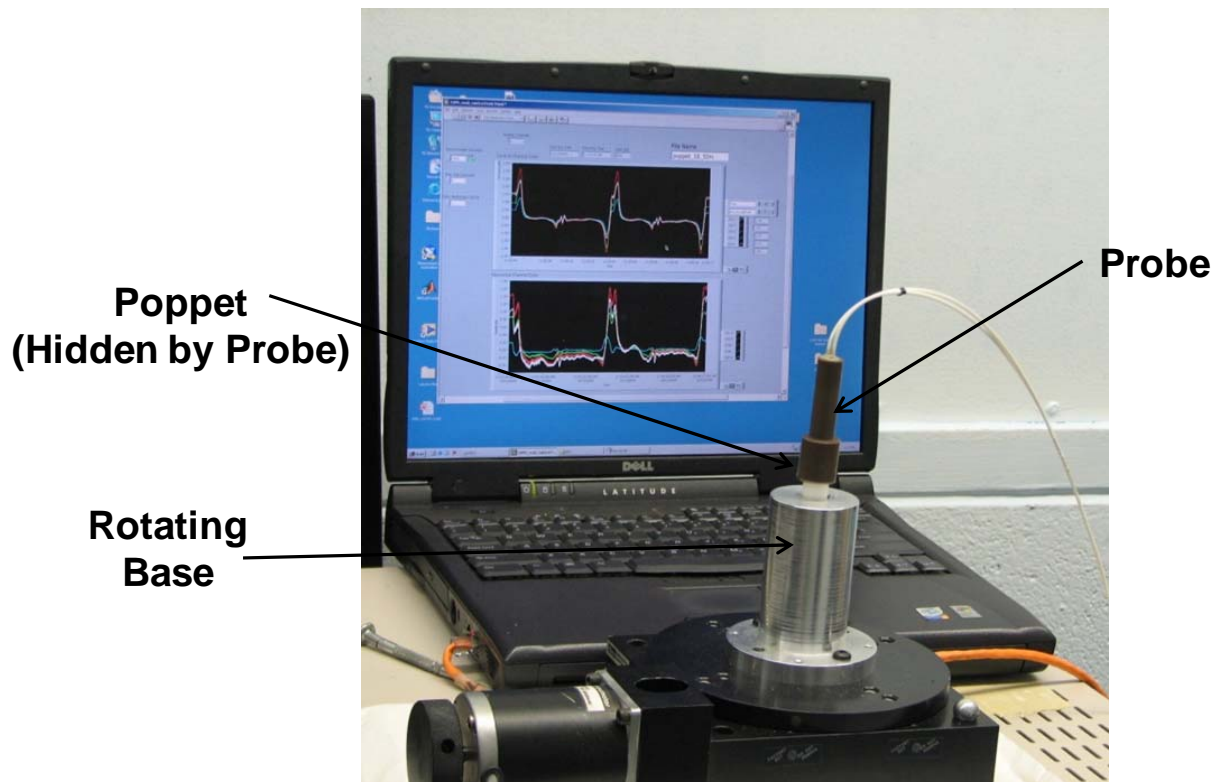
Crack inspection methods were used to detect the presence of cracks during the fatigue cycling and to characterize the size, shape, trajectory, location, and number of cracks in the poppet simulators. NDE characterization methods were used to detect cracks and measure the surface length, allowing the cracked poppet simulators to be used for the POD study. Destructive methods were used to characterize features like the crack shape, trajectory, and depth that were not visible from the poppet simulator surface.

#### 5.3.3.1 Laboratory EC Inspection


The manual method of crack generation required periodic interruption and inspection of the poppet simulator during the fatigue testing. A thorough SEM examination at each inspection interval was time and resource intensive, so a laboratory EC system was employed as a crack screening tool. The EC system consisted of a custom designed probe that fit over the poppet simulator and a mechanized base that rotated the simulator, as shown in Figure 5.3-7. The system rotated the poppet simulator twice in about two minutes and displayed the scan as a plot of voltage as a function of time. A baseline scan of the poppet simulator was performed prior to fatigue cycling and compared with subsequent scans obtained after fatigue cycling. The poppet simulator was returned to the loading fixture and cycling was continued if the scan did not show a significant change from the baseline. Cracks result in an oscillation of the voltage response,

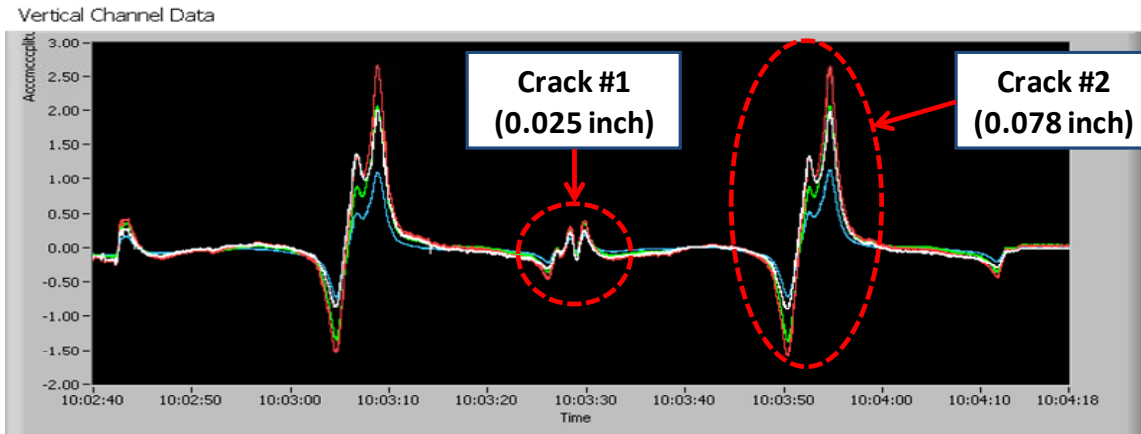
	<p align="center"><b>NASA Engineering and Safety Center Technical Assessment Report</b></p>	<p>Document #: <b>NESC-RP- 09-00506</b></p>	<p>Version: <b>1.1</b></p>
<p>Title: <b>STS-126 MPS#2 GH<sub>2</sub> Flow Control Valve Broken Poppet</b></p>		<p>Page #: 19 of 59</p>	

with an initial decrease as the probe first encounters the crack and an increase as the probe clears the crack, as shown in Figure 5.3-8. The magnitude of the voltage deviation is proportional to the size of the crack. The first signal of Figure 5.3-8 had a voltage deviation of about 1 volt and a 0.025 inch (0.64 mm) long crack was observed in the indicated location. The second signal of Figure 5.3-8 had a voltage deviation of about 4 volts and a 0.078 inch (2 mm) long crack was observed 180 degrees from the first indication. Fatigue cracks (~0.005 inches (0.13 mm)) exhibited a subtle voltage change that was barely larger than the background noise, so false calls were often observed when trying to generate small cracks. The laboratory EC inspection results were not included in the POD study because the device was not a controlled, field inspection system.



*Figure 5.3-7. Image of the EC System used to Screen the Poppet Simulators for Cracks*

	<b>NASA Engineering and Safety Center Technical Assessment Report</b>	Document #: <b>NESC-RP- 09-00506</b>	Version: <b>1.1</b>
		Title: <b>STS-126 MPS#2 GH<sub>2</sub> Flow Control Valve Broken Poppet</b>	




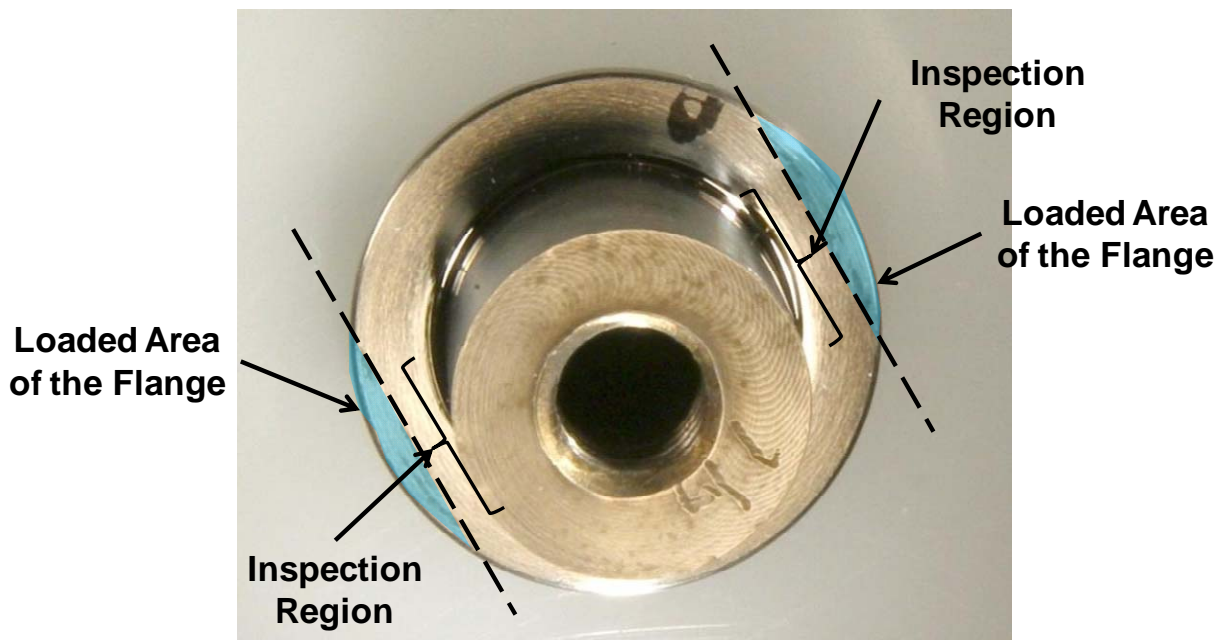
*Figure 5.3-8. EC Scan Result for a Poppet Simulator with Two Distinct Fatigue Cracks*

### 5.3.3.2 SEM Examination

A SEM was used to characterize the surface length, location, and number of fatigue cracks in each poppet. The poppets were polished, removing most of the manufacturing scratches, to aid in the location of the cracks. The SEM examination only considered the regions of the poppet simulator flange radius that were  $\pm 15$  degrees around the two primary loaded regions (0 and 180 degrees), as shown in Figure 5.3-9. The fatigue cracks exhibited small crack mouth openings in the unloaded state, making detection using the SEM difficult at low magnifications ( $< 100\times$ ). Examination at higher magnification ( $> 500\times$ ) was required to detect the fatigue cracks, which increased the inspection time by an order of magnitude. A repliset mold of the surface was made while the poppet simulator was loaded to 50 to 80 percent of the peak cyclic load. The repliset left a small amount of residual material at the crack mouth after the mold was removed and this residual material increased the crack detectability (due to surface charging), as shown in Figure 5.3-10. A low magnification examination was used to identify the location, number, and approximate crack size, and the remnant repliset material was removed by a  $\frac{1}{4}$  micron polish. The re-polished poppet simulators were examined with a high magnification SEM inspection of the known crack locations. SEM inspections of failed poppet simulators that were polished to remove the residual repliset material did not find any evidence of repliset on the fracture surfaces.



	<p align="center"><b>NASA Engineering and Safety Center Technical Assessment Report</b></p>	<p>Document #: <b>NESC-RP- 09-00506</b></p>	<p>Version: <b>1.1</b></p>
<p>Title: <b>STS-126 MPS#2 GH<sub>2</sub> Flow Control Valve Broken Poppet</b></p>		<p>Page #: 21 of 59</p>	



*Figure 5.3-9. Illustration of the High Stress Regions of the Poppet Simulators that were examined during the SEM Inspections*




**(a) With repliset (130x)**

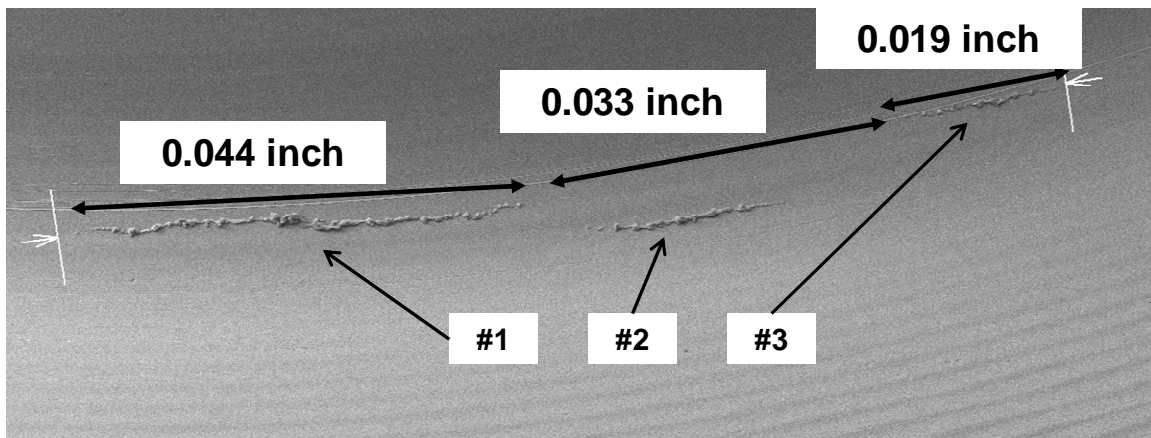
**(b) After polishing to remove repliset (90x)**

*Figure 5.3-10. SEM Images of a Crack in a Poppet Simulator with Repliset and after the Repliset has Been Removed*

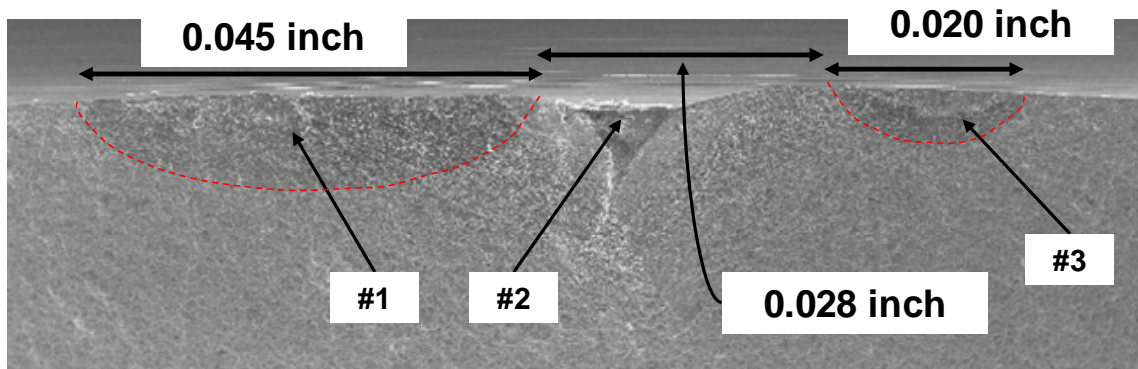
Several of the cracked poppets were fractured to reveal the fracture surface to allow characterization of the crack depth and shape. The initial attempts at destructive examination were performed by monotonically loading the cracked poppets to failure. A change in loading condition from fatigue crack growth to ductile fracture would often result in a distinct change in the fracture surface morphology that allows the size and shape of the fatigue crack to be measured. The change in fracture surface morphology for the material and loads used in this study was subtle and difficult to identify, so an alternative method of marking the end of the fatigue crack growth, or crack tip, was developed. This method consisted of placing the poppet

	<b>NASA Engineering and Safety Center Technical Assessment Report</b>	Document #: <b>NESC-RP-09-00506</b>	Version: <b>1.1</b>
Title: <b>STS-126 MPS#2 GH<sub>2</sub> Flow Control Valve Broken Poppet</b>		Page #: 22 of 59	

simulators in an oven that was preheated to 600°F and then increasing the temperature to 900°F over 20 minutes. The simulators were then removed and allowed to cool in air to oxidize the surface. The oxidized poppet simulators were then fatigue cycled at a stress ratio of  $R = 0.8$  and a peak load of 300 pounds until failure. The combination of crack surface oxidation and the change in cyclic loading resulted in a distinct change in the fracture surface morphology, as shown in Figure 5.3-11.



(a) Surface SEM examination of the intact poppet simulator




(b) Fracture surface SEM examination of the broken poppet simulator

Figure 5.3-11. Example of the Fracture Surface Morphology that Resulted from the Marking Process

## 5.4 Crack Characterization Results

There were 73 poppet simulators manufactured and 62 were successfully tested and characterized in terms of number of cracks, surface crack sizes, crack location relative to the 0 degree reference line, and crack location relative to other indications in the vicinity. Each poppet simulator had at most two regions of fatigue crack growth (the 0 and 180 degrees) locations. Some poppet simulators had crack growth in both regions (~68 percent) and the rest had crack growth in only one region (~32 percent). A total of 97 distinct high stress regions with at least one fatigue crack were found in the 62 poppets. Several of the poppet simulators failed

	<b>NASA Engineering and Safety Center Technical Assessment Report</b>	Document #: <b>NESC-RP- 09-00506</b>	Version: <b>1.1</b>
Title: <b>STS-126 MPS#2 GH<sub>2</sub> Flow Control Valve Broken Poppet</b>		Page #: 23 of 59	


prematurely during testing and several others were destructively examined for crack depth and shape measurements. Four poppet simulators that received no fatigue cycles and 51 poppet simulators with cracks were included in the POD analysis. The following sections describe the results from the examinations of the poppet simulator tests.

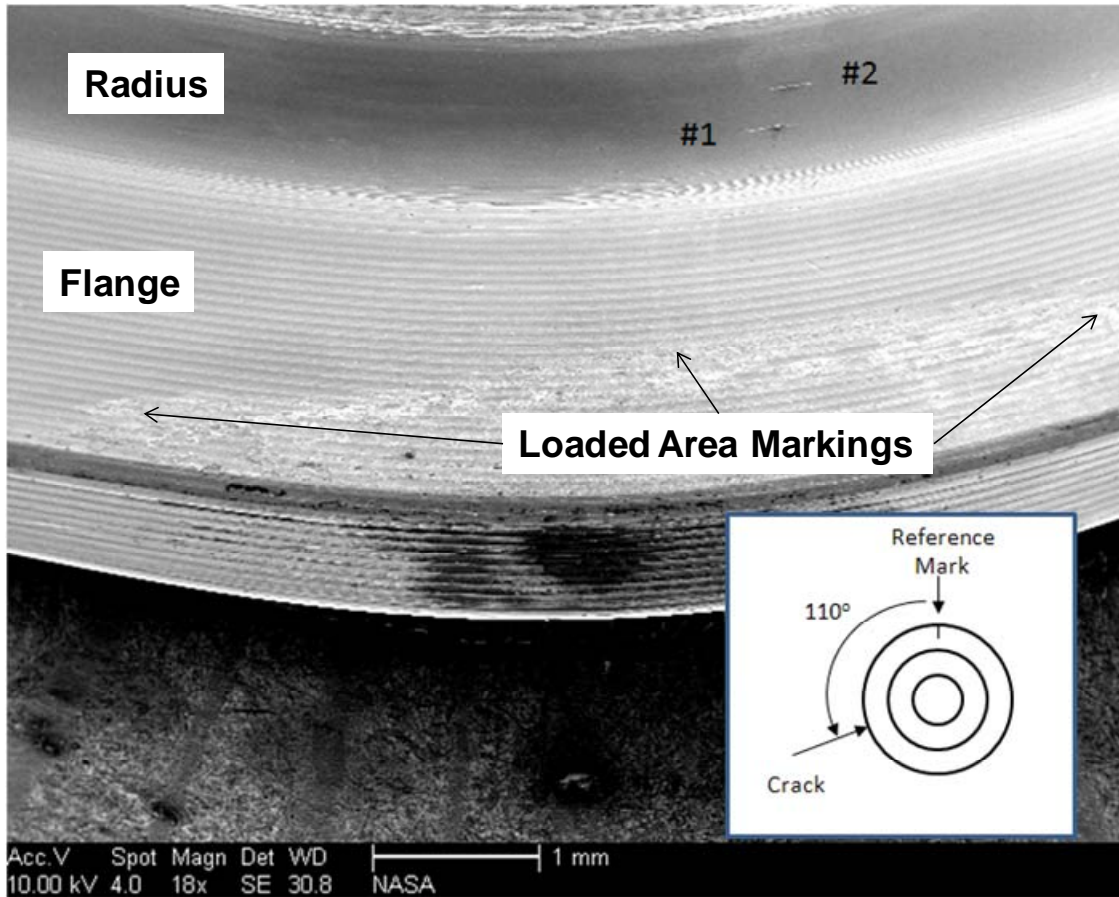
#### 5.4.1 SEM Surface Analysis

The flange radius of each poppet simulator was inspected with an SEM in a  $\pm 15$  degree arc around the 0 and 180 degree high stress regions. Each poppet simulator had a reference mark that was randomly selected so that the NDE inspectors would not deduce where the cracks were located. For example, an NDE reference mark at 70 degrees would rotate the 0 and 180 degree crack locations to 290 and 119 degrees, respectively in the new reference system. The NDE inspectors referenced the EC indications to the NDE reference mark.

The SEM examination initially located all of the cracks in the loading region. The example shown in Figure 5.4-1 contains two cracks that were located 110 degrees from the NDE reference mark (measured in a clockwise rotation). Examination at higher magnification was performed for each located crack, recording the surface lengths and distances to other cracks, as shown in Figure 5.4-2. An image record of every crack found in the tested poppet simulators is provided in Appendix A. The distribution of largest crack in each loading region is shown in Figure 5.4-3, and the number of cracks found in each poppet is summarized in Table 5.4-1.

The cracks that were located in the flight poppets were noted to have small crack openings, but no quantified measurements were provided. Crack opening displacements may influence the detectability of fatigue cracks, so the crack opening displacements were measured in several of the poppet simulators to quantify this parameter for the POD analysis. The crack opening displacement of the unloaded crack surfaces was characterized by examining several cracks at high magnification ( $\sim 10,000\times$ ). Several regions distributed along the crack length were documented at the high magnification and the separation of the two surfaces was measured at multiple locations, as illustrated in Figure 5.4-4. The crack opening displacement measurements were made for cracks with surface length from 0.005 to 0.136 inches (0.13 to 3.5 mm). As expected, the crack opening displacements were greatest in the center of the cracks and smallest at the crack tips. Most of the crack opening displacements were less than  $4 \times 10^{-5}$  inch (1 micron) and all of the crack opening displacements at the crack tips were less than  $8 \times 10^{-6}$  inch (0.2 micron), as shown in Figure 5.4-5.

	<p align="center"><b>NASA Engineering and Safety Center Technical Assessment Report</b></p>	<p>Document #: <b>NESC-RP-09-00506</b></p>	<p>Version: <b>1.1</b></p>
<p>Title: <b>STS-126 MPS#2 GH<sub>2</sub> Flow Control Valve Broken Poppet</b></p>		<p>Page #: 24 of 59</p>	



*Figure 5.4-1. Example of an SEM Image that shows the Location of Two Cracks*

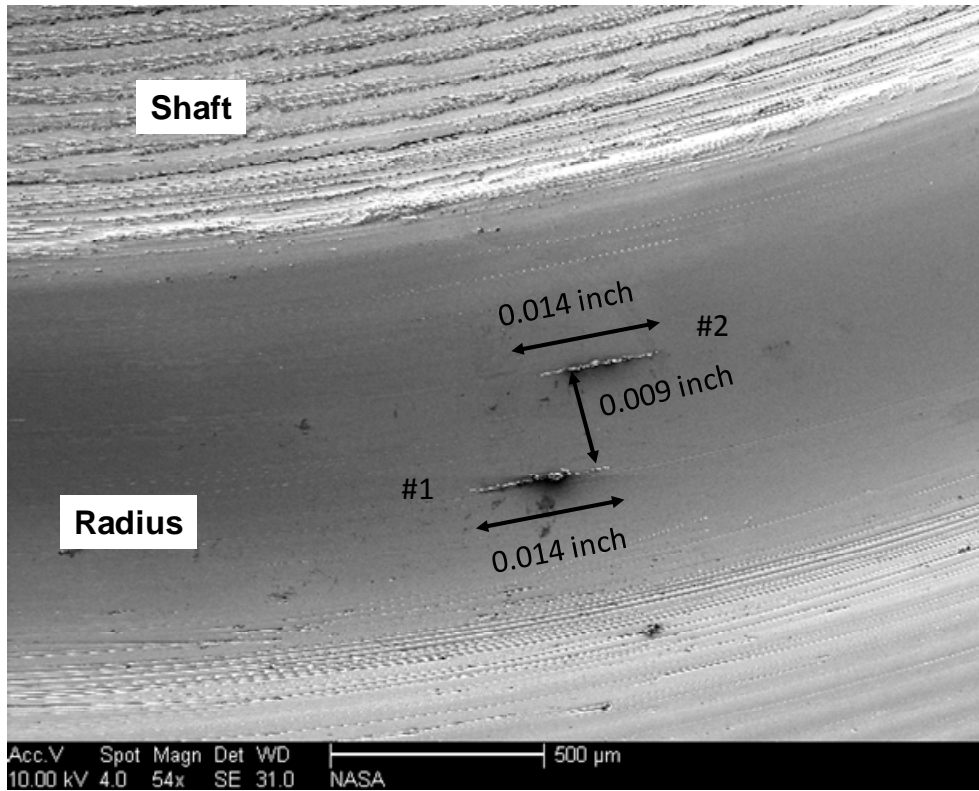


Figure 5.4-2. Example of an SEM image that shows Sufficient Details to Measure the Lengths and Relative Positions of Two Cracks

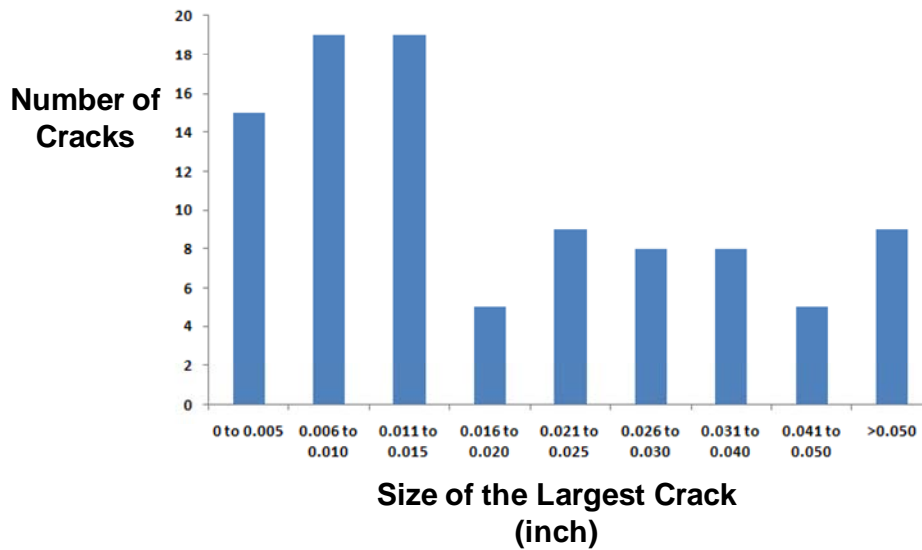
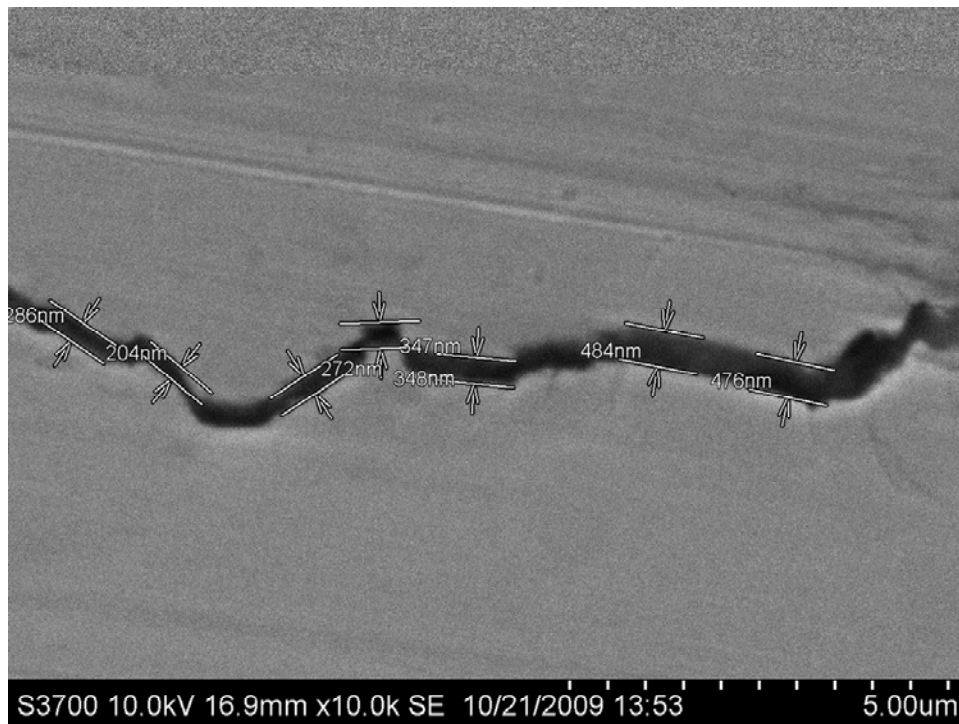


Figure 5.4-3. Distribution of the Largest Crack per Loaded Region of the Poppet Simulators Tested

*Table 5.4-1. Summary of the Number of Cracks Found in Each Poppet*

Type	Number	IDs
Singe Crack	10	11,12,14, 17, 23, 24, 27, 40, 53, 55
2 cracks (180-degrees apart)	4	7, <b>18</b> , 26, <b>51</b>
Single location with <5 cracks	7	13, 20, 21, 22, 29, 54, 60
4< cracks <9 (0° or 180°)	3	19, 38, 42
4< cracks <9 (0° and 180°)	11	33, <b>34</b> , <b>35</b> , <b>39</b> , 41, 47, 49, 57, 65, 66, 70
>8 cracks (0° or 180°)	1	37
>8 cracks (0° and 180°)	23	1, 31, 32, 36, 43, 44, 45, 46, 48, 50, 52, 56, 58, 59, 61, 62, 63, 64, 67, 68, 69, <b>71</b> , 72
No Cracks	3	16, 30, 73
<b>TOTAL</b>	<b>62</b>	

Note: The numbers highlighted in red indicate poppets that have been broken open for surface examination



*Figure 5.4-4. Image of a Poppet Crack at 10,000x Magnification with Crack Openings Measured at Several Locations*

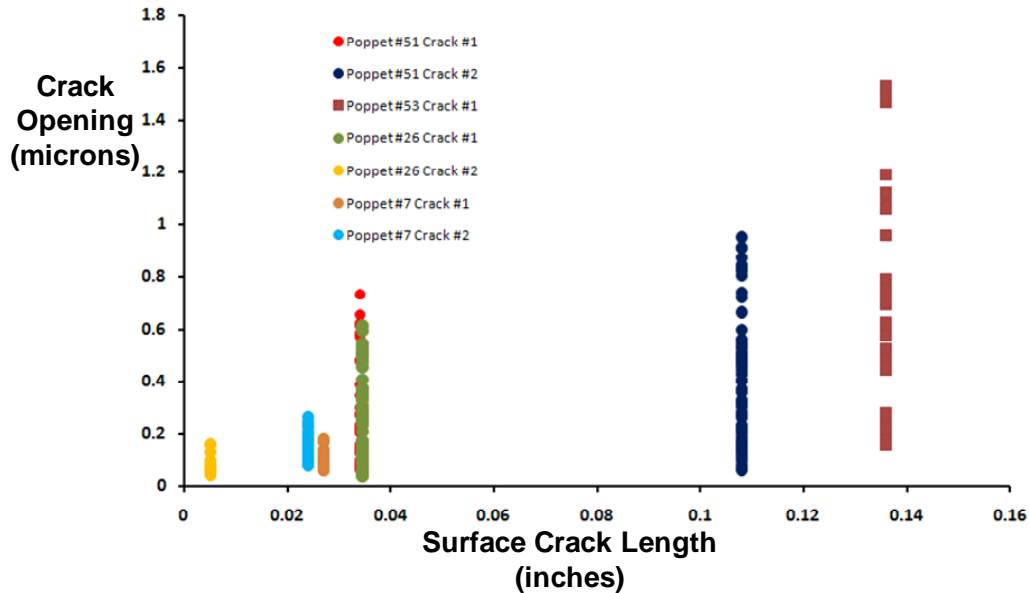



Figure 5.4-5. Crack Opening Displacement for Several Poppets

#### 5.4.2 Destructive Examination Results

The sensitivity of EC NDE methods may be related to the crack area, so several of the poppet simulators with fatigue cracks were destructively examined to determine the crack shape and depth. The destructive examination also provided verification that the surface crack lengths measured in the SEM examination were accurate. Five poppet simulators were destructively examined, revealing the shape of 16 cracks with surface lengths from 0.004 to over 0.13 inches (0.1 to 3.3 mm). The crack fronts were roughly semi-elliptical shaped, so the POD analysis could estimate the crack depth or crack area from the observed relationship between surface crack length and aspect ratio (ratio of crack depth to half surface crack length).

The process described in Section 5.3.3.2 was used to mark the crack front with both surface oxidation and fatigue cycling, and fracture with minimal plastic deformation of the surfaces. The failed surfaces were examined to determine if the cracks revealed by the destructive process could be correlated to the results of the non-destructive surface examination. The first check performed was to determine if the location of the cracks in the fracture surface matched with that observed on the poppet simulator surface. The presence of multiple cracks facilitated this check by allowing the measurement of the distance between the cracks. Figure 5.4-6 shows an example where three cracks were found on the surface of the intact poppet, but only two were revealed in the destructive examination. Cracks #4 and #6 appeared to be co-linear and about 0.05 inches (1.3 mm) apart and crack #5 appeared to be offset at a different location on the radius. The two cracks revealed in the destructive examination were 0.05 inches (1.3 mm) apart, suggesting that these cracks might be #4 and #6, whose coalescence during the high stress ratio fatigue cycling had bypassed crack #5. Comparisons of the crack lengths from the surface observations and from the destructive examination were performed, as shown in Figures 5.4-7


	<b>NASA Engineering and Safety Center Technical Assessment Report</b>	Document #: <b>NESC-RP- 09-00506</b>	Version: <b>1.1</b>
Title: <b>STS-126 MPS#2 GH<sub>2</sub> Flow Control Valve Broken Poppet</b>		Page #: 28 of 59	

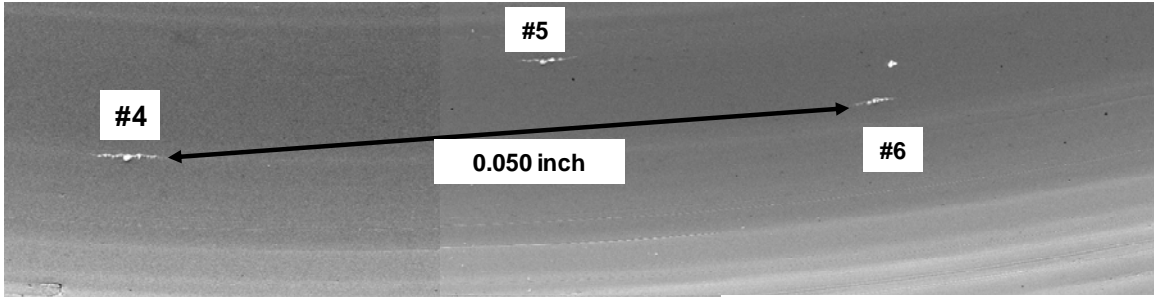
and 5.4-8, and both methods provided identical crack lengths. This provided additional evidence that the cracks found in the destructive examination were the same as cracks #4 and #6 from the observations from the intact surface. Furthermore, the agreement of the surface crack lengths measured in the nondestructive and destructive examinations indicate that the nondestructive examinations were accurately locating the crack tips, thus reporting accurate surface crack length measurements. The results from the destructive examination of the poppet simulators are provided in Appendix A of Volume II.

The crack depth and surface crack length were measured for 16 individual cracks from 5 poppet simulators that were destructively examined, as summarized in Table 5.4-2. The aspect ratio of crack depth to half surface crack length was calculated as a function of the surface crack length, as shown in Figure 5.4-9. Images of flight poppets from STS-126 revealed several crack fronts that indicated the crack size and shape at different points in time, as shown in Figure 5.4-10. Measurements of the surface crack length and crack depth were performed and the data was included in Figure 5.4-9. The measurements indicated that the cracks in the poppet simulators had a very similar shape (aspect ratio) as the cracks observed in the flight poppet. The measurements indicate that the smaller cracks were nearly semi-circular shaped, while the longer cracks became more elongated. A power law relationship was fit to the relationship between crack depth and surface crack length, as shown in Figure 5.4-11 and Equation 1.

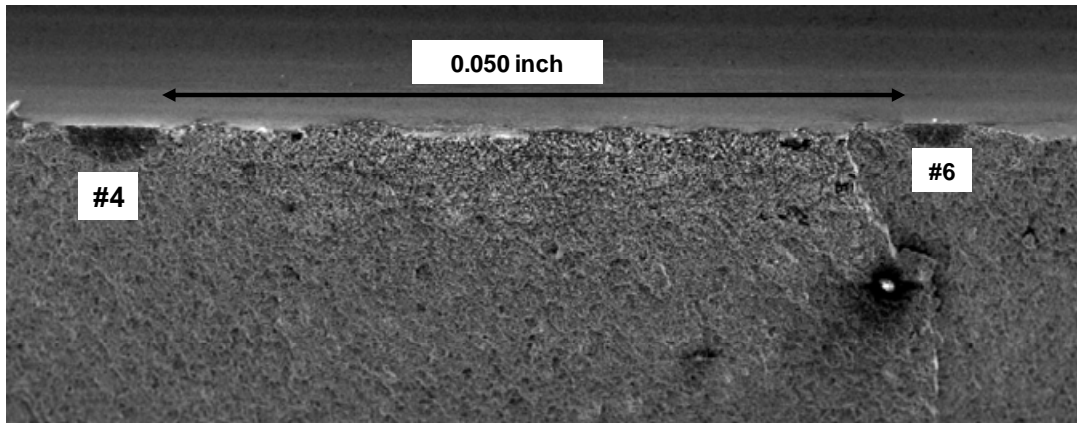
$$crack\ depth = 0.0823 \times (surface\ crack\ length)^{0.7021} \quad (1)$$



	<b>NASA Engineering and Safety Center Technical Assessment Report</b>	Document #: <b>NESC-RP-09-00506</b>	Version: <b>1.1</b>
Title: <b>STS-126 MPS#2 GH<sub>2</sub> Flow Control Valve Broken Poppet</b>		Page #: 29 of 59	

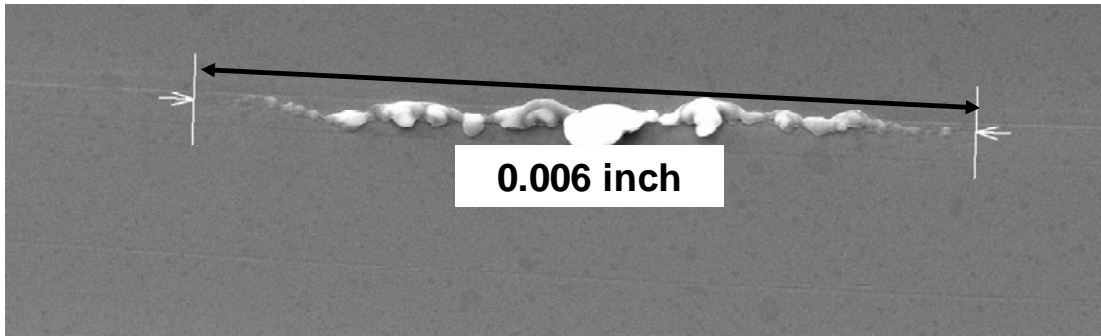


(a) Surface SEM examination of the intact poppet simulator

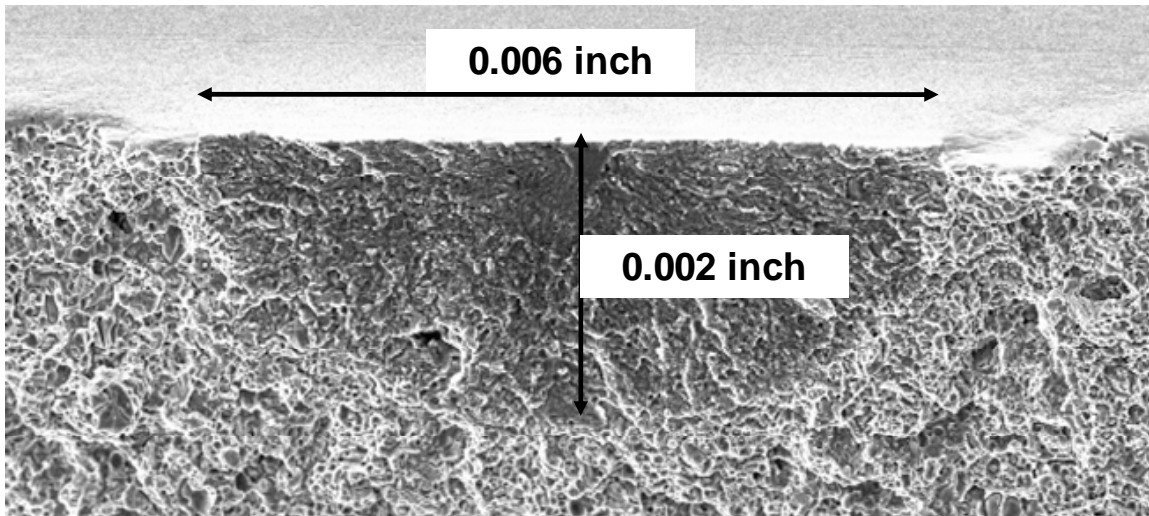


(b) Fracture surface SEM examination of the broken poppet simulator

*Figure 5.4-6. Images of a Fracture Surface from a Poppet Simulator and the Cracks observed on the Surface prior to Destructive Examination*

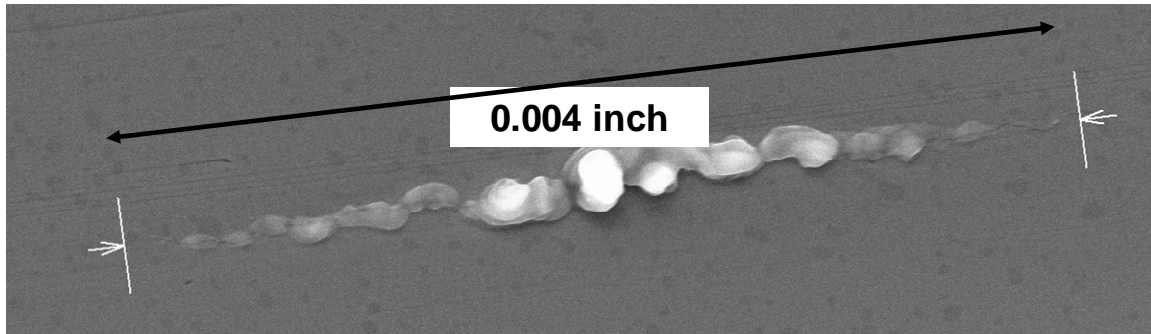


**(a) Surface SEM examination of the intact poppet simulator**

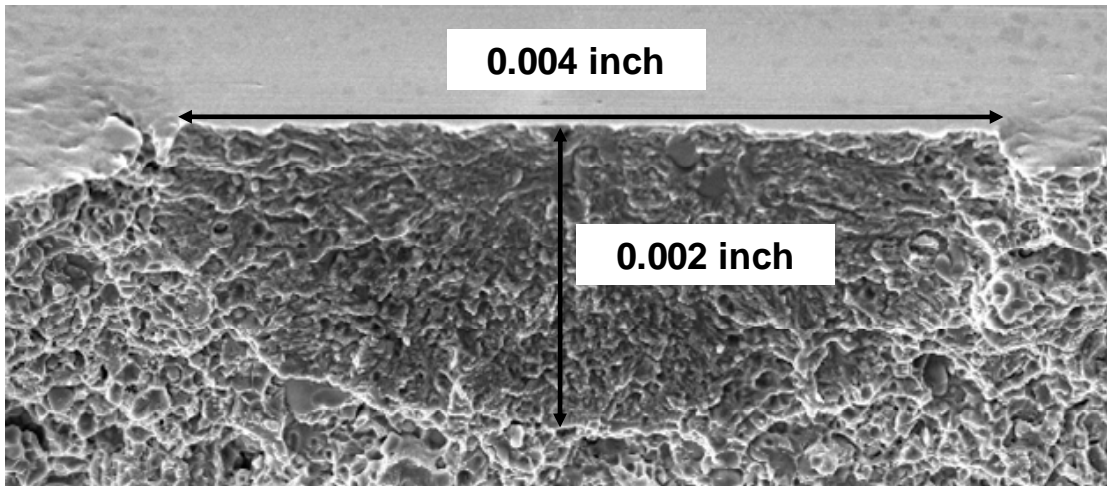


**(b) Fracture surface SEM examination of the broken poppet simulator**

*Figure 5.4-7. Comparison of the Surface Crack Length Measured and after Destructive Examination of crack #4 from Figure 5.4-6*



**(a) Surface SEM examination of the intact poppet simulator**



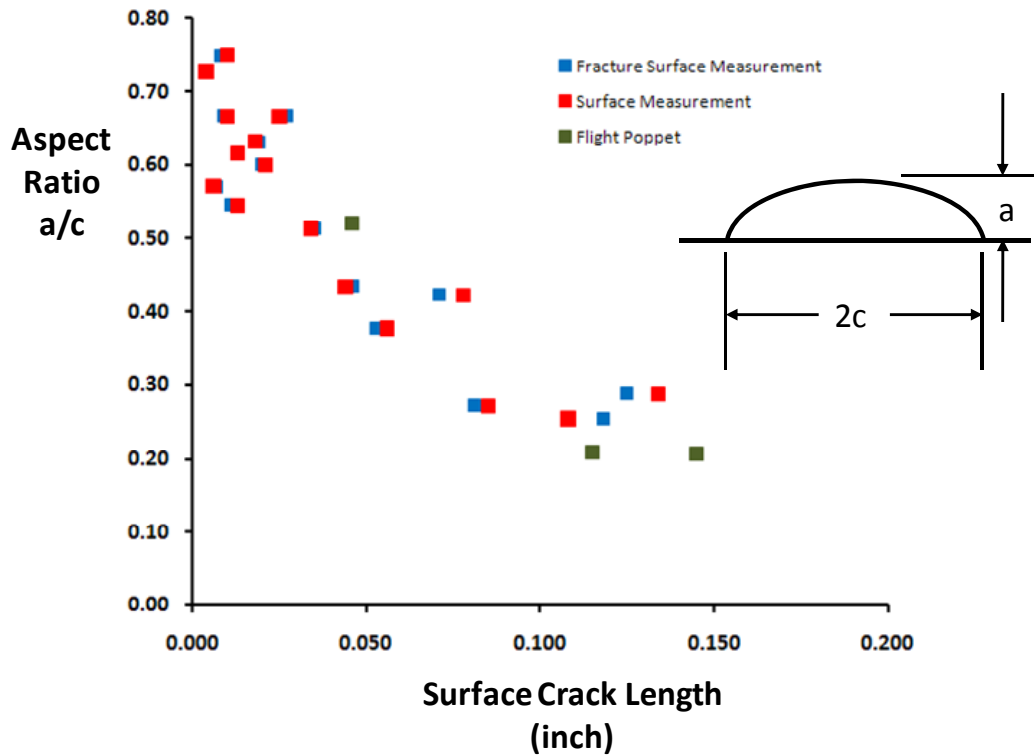
**(b) Fracture surface SEM examination of the broken poppet simulator**

*Figure 5.4-8. Comparison of the Surface Crack Length Measured and after Destructive Examination of Crack #6 from Figure 5.4-6*




*Table 5.4-2. Summary of the Crack Depth Measurements from the Poppet Simulators that were Destructively Examined*

Poppet #	Crack #	SEM Surface Length, 2c (inch)	Fracture Surface Length, 2c (inch)	Fracture Surface Depth, a (inch)	Fracture Surface a/c
34	1	0.134	0.125	0.018	0.29
34	2a	0.013	0.013	0.004	0.62
34	2b	0.013	0.011	0.003	0.55
34	3	0.010	0.008	0.003	0.75
34	4	0.021	0.020	0.006	0.60
39	1	0.085	0.081	0.011	0.27
39	2	0.010	0.009	0.003	0.67
39	3	0.056	0.053	0.010	0.38
35	1	0.044	0.046	0.010	0.43
35	3	0.018	0.019	0.006	0.63
35	4	0.006	0.007	0.002	0.57
35	6	0.004	0.004	0.002	0.73
18	1	0.078	0.071	0.015	0.42
18	2	0.025	0.027	0.009	0.67
51	2	0.108	0.118	0.015	0.25
51	1	0.034	0.035	0.009	0.51

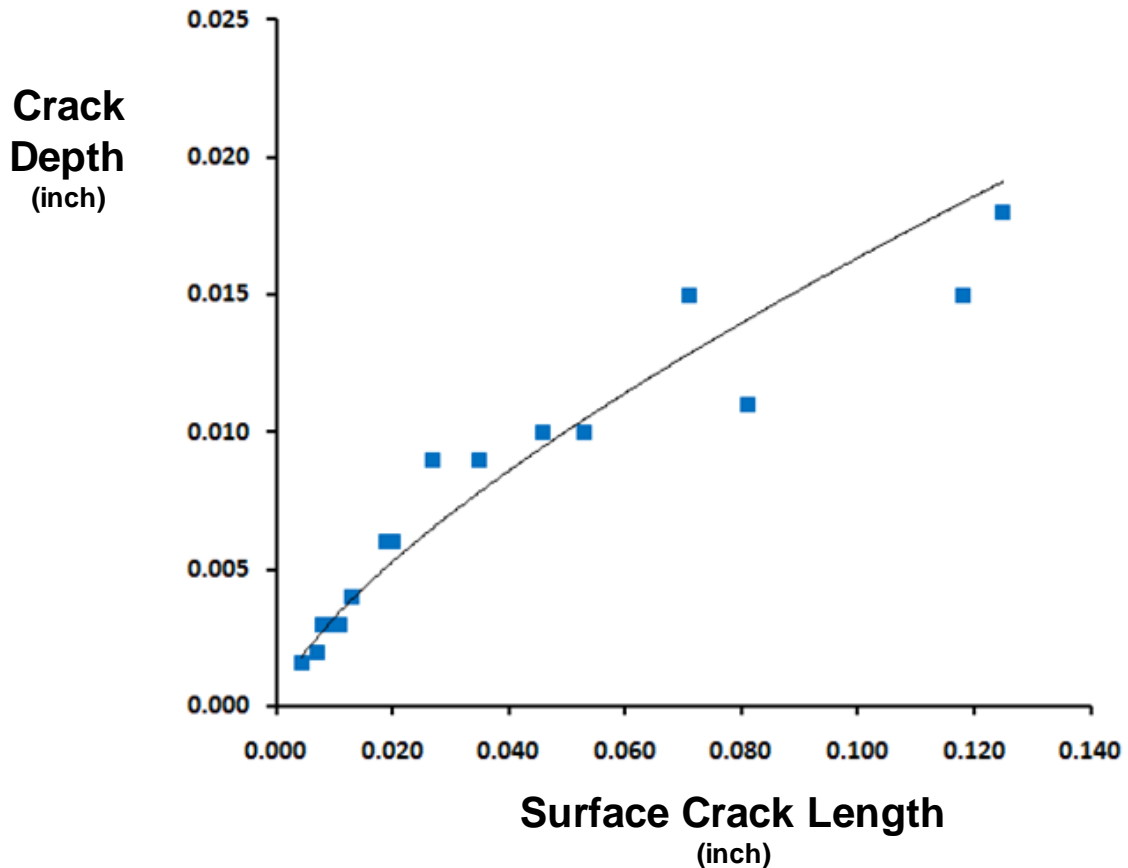


*Figure 5.4-9. Aspect Ratio of several Cracks from Poppet Simulators and Flight Poppets obtained from the Destructive Examinations*

	<b>NASA Engineering and Safety Center Technical Assessment Report</b>	Document #: <b>NESC-RP- 09-00506</b>	Version: <b>1.1</b>
Title: <b>STS-126 MPS#2 GH<sub>2</sub> Flow Control Valve Broken Poppet</b>		Page #: 33 of 59	




*Figure 5.4-10. Image of the Crack Detected in Flight Poppet from STS-126*



*Figure 5.4-11. Measured Crack Depth from the Destructive Examinations as a Function of the Surface Crack Length*

## 5.5 EC Simulated Poppet POD Testing and Analysis

EC inspections were performed on 55 of the poppet simulators, described in the preceding sections, to acquire the data necessary for the POD analysis. The inspections were performed by the two Boeing Company Huntington Beach inspectors responsible for the inspection of flight FCV poppets. To ensure a “blind” inspection procedure, all poppet simulators were inspected


	<b>NASA Engineering and Safety Center Technical Assessment Report</b>	Document #: <b>NESC-RP- 09-00506</b>	Version: <b>1.1</b>
Title: <b>STS-126 MPS#2 GH<sub>2</sub> Flow Control Valve Broken Poppet</b>		Page #: 34 of 59	

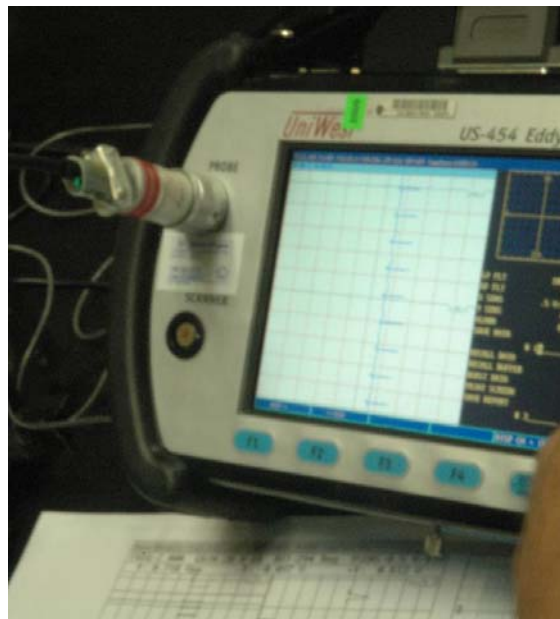
with no information as to crack size or location. In addition, four poppet simulators containing no cracks (control simulators) were randomly submitted for inspection. The inspections were performed according to the established Boeing Company Eddy Current Procedure/Technique Sheet Flow Control Valve Poppet - #SSO-01 Revision C. A copy of the procedure is included as Appendix B with only one modification; the inspectors were instructed not to use any specific threshold signal value to determine crack indications, but instead to identify all crack-like signal indications regardless of the signal magnitude. This allowed the POD analysis to be performed independent of a threshold to estimate the smallest size cracks that could be detected with 90/95 POD. Both inspectors repeated the inspection on each poppet simulator six times to provide data on operator repeatability.

A poppet rotation device and a probe holder with controlled degrees of freedom were needed to establish a repeatable EC data acquisition process. A UniWest US 1779 bolt rotation device (Figures 5.5-1 and 5.5-2) and probe holder was the selected for this purpose. This configuration used a model US 1779 bolt rotation device/scanner and a model US 1839 probe (Figure 5.5-3). The probe tip has an included angle of 60 degree and a radius of 0.03125 inch (0.8 mm). The design allows the probe to contact the root of a bolt thread for detection of cracks at the thread root. The probe has two coils in a driver pick-up arrangement and their centers are separated by approximately 0.1 inch (2.54 mm). This configuration was used to inspect flight poppets and the popper simulators in the POD study.

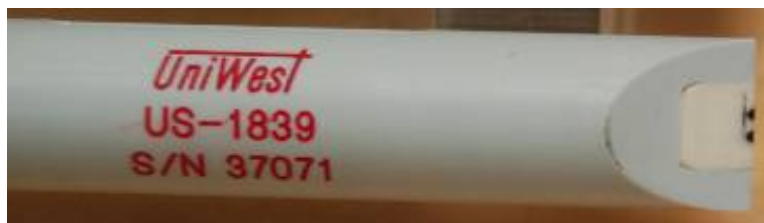


*Figure 5.5-1. US 1779 (UniWest) Bolt Inspection Scanner*

	<p align="center"><b>NASA Engineering and Safety Center Technical Assessment Report</b></p>	<p>Document #: <b>NESC-RP- 09-00506</b></p>	<p>Version: <b>1.1</b></p>
<p>Title: <b>STS-126 MPS#2 GH<sub>2</sub> Flow Control Valve Broken Poppet</b></p>		<p>Page #: 35 of 59</p>	




*Figure 5.5-2. US 454 (UniWest) EC Crack Detector*



*Figure 5.5-3. EC Bolt Thread Root Inspection Probe US 1839*

The 440A poppet material is a ferromagnetic martensite steel with an electrical resistivity of 0.5 percent International Annealed Copper Standard (IACS), a maximum relative permeability of 60, and a coercive force of approximately 65 Oersted. The relative magnetic permeability was about 25 at a demagnetized (or a very low magnetized) state. The magnetic properties were verified at the NASA Langley Research Center (LaRC) NDE Laboratory. The magnetic properties indicate that the material was mildly ferromagnetic and held residual magnetism (~1 Gauss) after an ambient demagnetization. A variation in microstructure may cause some variation in magnetic permeability and the residual stress and cold work (strain) could also cause the magnetic permeability to change in some ferromagnetic steels. The poppet operational environment constitutes surface flow of GH<sub>2</sub> at a certain pressure, temperature and rate; and exposure to various vibration modes and acoustic waves generated due to gas flow as well as from external sources. Flight poppets are also subjected to a magnetic force from the FCV solenoid. It is suspected that the poppet operational environment may cause changes in the

	<b>NASA Engineering and Safety Center Technical Assessment Report</b>	Document #: <b>NESC-RP- 09-00506</b>	Version: <b>1.1</b>
Title: <b>STS-126 MPS#2 GH<sub>2</sub> Flow Control Valve Broken Poppet</b>		Page #: 36 of 59	

magnetic permeability that could affect the EC response. Thus, the EC technique needs to be sensitive to detect cracks in the presence of any potential permeability range and variability at the inspection site.

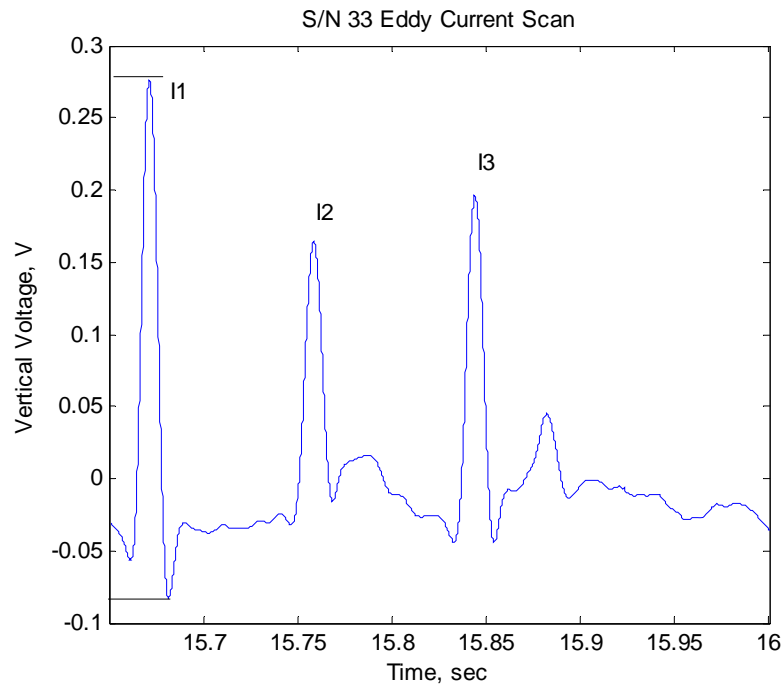
A frequency of 2 MHz was selected to optimize the detection of shallow cracks (0.005 inches (0.13 mm)). An electro-discharged machined (EDM) notch standard was fabricated from flight S/N 33-361 poppet (Figure 5.5-4). Note that any change in the magnetic permeability at notches due to the EDM process was not characterized. The notch dimensions were 0.030 long x 0.015 deep x 0.005 inch wide (0.76 x 0.38 x 0.13 mm). Three circumferential notches of the same size were machined in poppet S/N 33-361; the first notch was located at the center of the radius, the second was located at the radius tangential point with the shank, and the third notch was located at the radius tangential point with the flange.



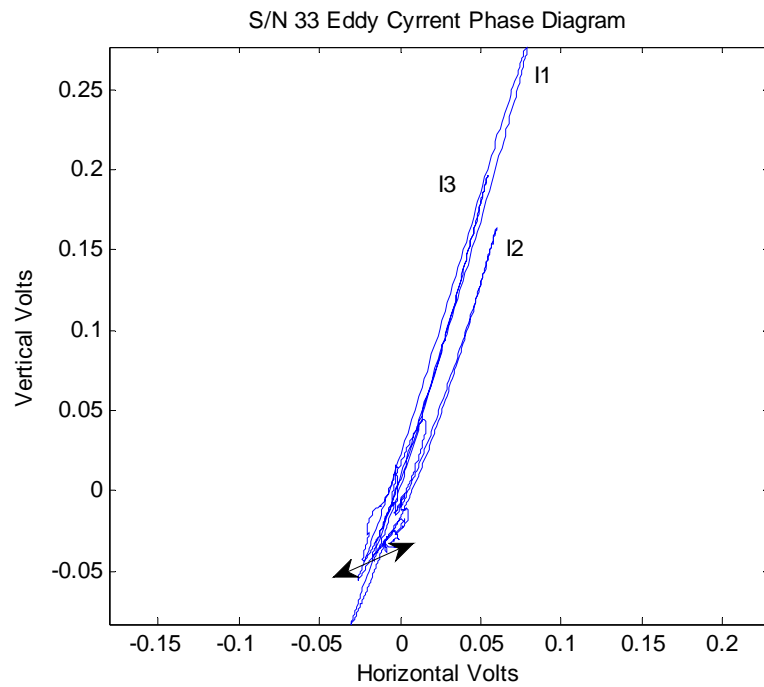
*Figure 5.5-4. S/N 33 Poppet Standard*

The voltage scan and phase diagrams were obtained from the EC responses for the three EDM notches of poppet S/N 33-361, as shown in Figures 5.5-5 and 5.5-6, respectively. The peak-to-peak voltage ( $V_{pp}$ ) was the difference (0.36  $V_{pp}$ ) between the two horizontal lines that bracket the I1 indication in Figure 5.5-5. Scanning of the EC probe causes a slight back and forth movement that causes lift-off of the probe coil relative to the contact surface. The EC response changes along a particular direction in the phase diagram due to this lift off, as indicated by the double arrow in phase diagram of Figure 5.5-6. Crack indications will appear as a sharp increase in the voltage scan and will have tight phase loops that point towards 1 to 2 o'clock on the phase diagram. Poppet S/N 33-361 also has a smaller crack-like indication to the right of the I3 peak and a non-crack-like indication between the I2 and I3 peaks in the voltage scan of Figure 5.5-5. However, the magnitude of these additional signals is small in relation to the typical background noise level and they have not been associated with additional detected cracks or defects.






*Figure 5.5-5. EC Voltage Scan of S/N 33-361 Standard*



*Figure 5.5-6. EC Phase Diagram of S/N 33-361 Standard*

	<b>NASA Engineering and Safety Center Technical Assessment Report</b>	Document #: <b>NESC-RP- 09-00506</b>	Version: <b>1.1</b>
Title: <b>STS-126 MPS#2 GH<sub>2</sub> Flow Control Valve Broken Poppet</b>		Page #: 38 of 59	

A non-magnetic (titanium) bolt standard (1 percent IACS) was used for verification of the technique sensitivity. The response from the titanium standard was slightly different from the A440 steel, but comparable in phase and amplitude to the response from the S/N 33-361 standard and the cracks in 440A poppet simulators. The EC setup was verified before and after the EC test on the titanium standard. The EC inspections were performed after demagnetizing the poppet or verifying that the magnetic field was less than 1 Gauss to minimize the effect of the residual magnetic field on the EC response.

The results from the multiple EC inspections on the simulated poppet by both inspectors, listed in Appendix A, were used as input for the POD analysis for the EC inspection process for poppets. Additionally, a statistical analysis of the variation in signal responses for multiple inspections and across the different inspectors was performed to understand measurement variability. These results were used to establish additional criteria for crack indications based on changes in signal response before and after poppet usage (e.g., flow balancing, flight operations). The first POD model was an analysis of the crack “calls” and “no calls” made after the EC poppet simulator inspections. Additional analyses were performed based on the specific signals ( $V_{pp}$ ) obtained by the inspectors for each poppet simulator. The POD curves were derived from regression models that used different explanatory variables (e.g., largest crack size, cumulative crack length, total crack area).

A total of 55 poppet simulators (including 4 “control” uncracked poppet simulators) were examined by the two inspectors. The cracked poppet simulators had either one region with cracks or two diametrically opposed regions with cracks. The number of cracks in an individual region varied from 1 to more than 20. Note the two inspectors were not given any information relative to the number of cracks contained in the simulators or crack location. The initial characterization of the cracked poppet simulators was in terms of the number of cracks and the largest crack contained on the diametrically opposed loading regions of the poppet simulators. The diametrically opposed loading allowed the analyses to consider two inspection results from each poppet. A summary of the SEM crack findings and the EC inspection results from Inspector 1 and 2 are provided in Table 5.5-1. The largest crack found in each loading region, and the total number of cracks identified, are reported along with the measured  $V_{pp}$  voltages and a crack indication (“Y”, “N”, or “Poss.”) for each inspector. Inspector 1 identified several crack indications as “possible crack start”, hence the “Poss.” designation in Table 5.5-1. The highlighted cells in Table 5.5-1 indicated false calls and missed cracks.

The distribution of the number of cracked regions reported by the inspectors and the number of crack regions reported by the SEM examination are provided in Table 5.5-2. For example, the SEM examination determined that 32 poppet simulators had cracks in both loading regions, while Inspector 2 reported: no cracks on two; located cracks in only a single loading region on 18; and located cracks in both loading regions on 12 of these 32 poppet simulators. Note that an inspector reporting a  $V_{pp}$  signal response did not necessarily indicate that it was an indication of a crack. The data from Inspector 1 contained several cases of responses designated as “possible crack start”, indicating that the signal was stronger than the background noise, but did not meet the 3:1 signal to noise ratio criterion needed to be identified as a crack.



# NASA Engineering and Safety Center Technical Assessment Report

Document #:  
**NESC-RP-  
09-00506**

Version:  
**1.1**

Title:

**STS-126 MPS#2 GH<sub>2</sub> Flow Control Valve Broken Poppet**

Page #:  
39 of 59

*Table 5.5-1. Summary of SEM Characterization and Inspection Findings*

Poppet	Loading Region with the Largest Crack						Diametrical Opposite Loading Region					
	Largest Crack (inch)	Total Cracks	Inspector 1		Inspector 2		Largest Crack (inch)	Total Cracks	Inspector 1		Inspector 2	
			Average Vpp	Crack Call	Average Vpp	Crack Call			Average Vpp	Crack Call	Average Vpp	Crack Call
1	0.018	5	0.157	Y	0.148	Y	0.007	4	-	N	-	N
4	-	0	0.024	N	0.031	N	-	0	-	N	-	N
7	0.027	2	0.248	Y	0.236	Y	0.024	1	0.137	Y	0.197	Y
11	0.075	1	1.127	Y	1.076	Y	-	0	-	N	-	N
12	0.041	1	0.588	Y	0.661	Y	-	0	-	N	-	N
13	0.014	1	0.198	Y	0.189	Y	-	0	-	N	-	N
14	0.033	1	0.420	Y	0.438	Y	-	0	0.039	Poss.	-	N
16	-	0	0.153	Y	0.124	Y	-	0	-	-	-	-
17	0.026	1	0.275	Y	0.263	Y	-	0	-	N	-	N
18	0.078	1	1.063	Y	1.055	Y	0.025	1	0.248	Y	0.259	Y
19	0.037	5	0.512	Y	0.509	Y	-	0	-	N	-	N
20	0.017	3	0.151	Y	0.148	Y	-	0	-	N	-	N
21	0.017	5	0.142	Y	0.135	Y	-	0	-	N	-	N
22	0.022	3	0.227	Y	0.225	Y	-	0	-	N	-	N
23	0.026	1	0.195	Y	0.183	Y	-	0	-	N	-	N
24	0.012	1	0.087	Y	0.091	Y	-	0	-	N	-	N
26	0.034	1	0.357	Y	0.359	Y	0.005	1	-	N	-	N
27	0.032	1	0.444	Y	0.462	Y	-	0	-	N	-	N
29	0.038	4	0.540	Y	0.562	Y	-	0	-	N	-	N
30	-	0	0.051	N	0.062	N	-	0	-	N	-	N
31	0.015	10	0.231	Y	0.226	Y	0.002	1	-	N	-	N
32	0.025	6	0.247	Y	0.245	Y	0.012	3	0.080	Y	0.071	Y
33	0.026	4	0.222	Y	0.214	Y	0.003	1	-	N	-	N
34	0.134	1	0.684	Y	0.670	Y	0.036	3	0.233	Y	0.217	Y
35	0.044	3	0.590	Y	0.575	Y	0.006	2	0.070	Poss.	-	N
36	0.014	17	0.160	Y	0.158	Y	0.009	3	0.092	Y	0.076	Y
37	0.022	3	0.249	Y	0.259	Y	0.002	3	0.055	Poss.	-	N
38	0.078	1	0.900	Y	0.895	Y	0.014	2	0.077	Y	0.081	Y
39	0.084	2	1.005	Y	0.968	Y	0.059	2	0.667	Y	0.641	Y
40	0.010	1	0.080	Y	-	No Data	-	0	-	N	-	No Data
41	0.055	4	0.802	Y	0.821	Y	0.002	1	-	N	-	N
42	0.025	5	0.243	Y	0.265	Y	-	0	0.043	Poss.	-	N
43	0.012	21	0.147	Y	0.148	Y	0.003	6	0.044	Poss.	-	N
44	0.038	7	0.270	Y	0.275	Y	0.009	2	0.043	Poss.	-	N
45	0.014	1	0.080	Y	0.065	Y	0.009	4	0.079	Y	0.088	Y
46	0.012	10	0.098	Y	0.101	Y	0.006	9	0.069	Poss.	-	N
47	0.014	6	0.141	Y	0.144	Y	0.004	1	0.059	Poss.	-	N
48	0.041	11	0.353	Y	0.344	Y	0.004	2	-	N	-	N
49	0.045	5	0.807	Y	0.822	Y	0.002	1	-	N	-	N
50	0.022	5	0.212	Y	0.209	Y	0.005	4	0.057	Poss.	-	N
51	0.108	1	1.045	Y	1.064	Y	0.032	1	0.419	Y	0.419	Y
52	0.033	8	0.221	Y	0.218	Y	0.015	7	0.099	Y	0.095	Y
53	0.136	1	1.115	Y	1.106	Y	-	0	-	N	-	N
54	0.017	2	0.212	Y	0.219	Y	-	0	-	N	-	N
55	0.004	1	0.041	N	0.035	N	-	0	-	N	-	N
57	0.087	5	0.485	Y	0.484	Y	0.006	3	0.168	Y	0.163	N
60	0.037	6	0.610	Y	0.611	Y	-	0	-	N	-	N
61	0.018	13	0.193	Y	0.203	Y	0.016	15	0.176	Y	0.177	Y
64	0.025	14	0.240	Y	0.242	Y	0.004	6	0.069	Poss.	-	N
65	0.004	3	0.077	N	0.081	N	0.002	3	-	N	-	N
66	0.025	4	0.187	Y	0.191	Y	0.005	1	-	N	-	N
67	0.009	7	0.091	Poss.	0.097	N	0.007	8	-	N	-	N
68	0.025	8	0.210	Y	0.220	Y	0.012	6	0.124	Y	0.121	Y
70	0.016	3	0.179	Y	0.185	Y	0.008	2	0.099	Poss.	0.099	N
73	-	0	0.068	N	0.096	N	-	0	-	N	-	N

**Table 5.5-2. Number of Loaded Regions with Known Cracks and the Reported Responses**

Sides Reported	SEM: Cracks on one side		SEM: Cracks on two sides		Dummy Simulators	
	Inspector 1	Inspector2	Inspector 1	Inspector2	Inspector 1	Inspector2
0	1	1	1	2	3	3
1	16	17	10	19	1	1
2	2	0	21	11	0	0
No Data	0	1	0	0	0	0
Total	19	19	32	32	4	4

### 5.5.1 Hit/Miss Analysis


The first POD analysis was performed on the individual calls made by the inspectors versus the largest crack length in a cracked region. The data were analyzed as if the two loaded regions of a poppet simulator were independent inspections. Thus, from the SEM characterizations there were a total of 83 data points (19 + 2x32) from cracked regions. The loaded regions that were found to have cracks by the SEM characterization, but did not have a crack response indicated by the inspectors were considered as a “no call.”

Table 5.5-3 contains a summary of the calls made by each inspector. The number of times Inspector 1 made a “possible crack start” call was denoted as “Poss.” Both inspectors reported crack indications for all loading regions where the largest crack was 0.010 inches (0.25 mm) or greater. The inspectors only reported a few “possible” crack indications and no “hits” (unambiguous crack indications) in the loaded regions where the largest crack was 0.005 inches (0.13 mm) or smaller. The loaded regions with the largest crack in the range of 0.006 to 0.009 inches (0.15 to 0.23 mm) were where the mixed (crack/no crack) results occurred and where the rise in the estimated POD curve was expected to occur.

**Table 5.5-3. Inspection Findings Based on the Largest Crack Length in a Loading Region**

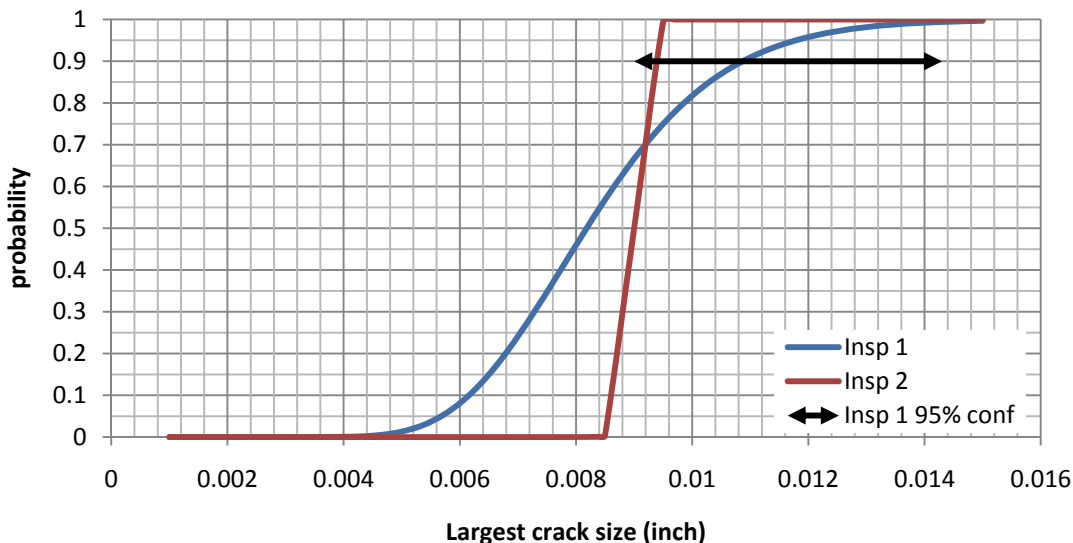
Inspector	Largest Crack Length in a Loading Region (inch)										Total Loading Regions
	No Crack			0.001 to 0.005		0.006 to 0.009			> 0.009		
	False	No	Poss.	No	Poss.	No	Poss.	Crack	Crack	No Data	
1	1	24	2	12	3	2	5	3	58	0	110
2	1	26	0	15	0	8	0	2	57	1	110

The “Poss.” calls from Inspector 1 were considered as no calls in the fitting of the POD curves to the hit/miss data, because the indications violate the 3:1 signal to noise criteria, and violating that criteria would likely result in an increase in the number of false calls. Figure 5.5-7 shows the estimated curves from the model  $POD(a) = \Phi(c + d \cdot \ln(a))$ , where  $\Phi$  is the standard Gaussian cumulative distribution function,  $a$  is the crack size, and  $c$  and  $d$  are fit parameters. As expected, the mixed region of hits and misses was in the range where the largest crack was between 0.006 and 0.009 inches (0.15 to 0.23 mm). Table 5.5-3 indicates that Inspector 1 had 3 hits and 7 misses, whereas Inspector 2 had 2 hits and 8 misses. Intuition might suggest that Inspector 1 would have a “better” estimated POD curve. The three hits of Inspector 1 were for loaded regions where the largest cracks were 0.006 and 0.009 inches (0.15 to 0.23 mm), whereas

	<b>NASA Engineering and Safety Center Technical Assessment Report</b>	Document #: <b>NESC-RP-09-00506</b>	Version: <b>1.1</b>
Title: <b>STS-126 MPS#2 GH<sub>2</sub> Flow Control Valve Broken Poppet</b>		Page #: 41 of 59	


of the two hits from Inspector 2 were for loaded regions where the largest crack was 0.009 inches (0.23 mm). There were a total of 4 loaded regions where the largest crack was 0.009 inches (0.23 mm) and therefore a maximum likelihood fit to Inspector 2 data is a steep curve going through probability of 0.5 at 0.009 inches (12.7 to 0.23 mm). That is, the likelihood is maximized as long as the curve is essentially 0 at 0.008 inches (0.20 mm), 1 at 0.010 inches (0.25 mm), and 0.5 at 0.009 inches (0.23 mm). However, the overlap of crack lengths for the 2 hits of Inspector 1 induces more variation in the estimate, translating to a higher estimate for the crack lengths corresponding to the higher probabilities. The net result was that for the purposes of making a confidence statement for the crack length corresponding to a POD of 0.9, it was more conservative to use the inspection results of Inspector 1. The confidence bounds shown in Figure 5.5-7 were based on likelihood ratio statistics and the maximum likelihood fit that yielded a POD function estimate of  $POD(a) = \Phi(21.6903 + 4.51314 * \ln(a))$ . Here,  $\Phi(\cdot)$  was the standard Gaussian distribution function and  $a$  was the crack length in inches.

### Estimated POD for hit/miss



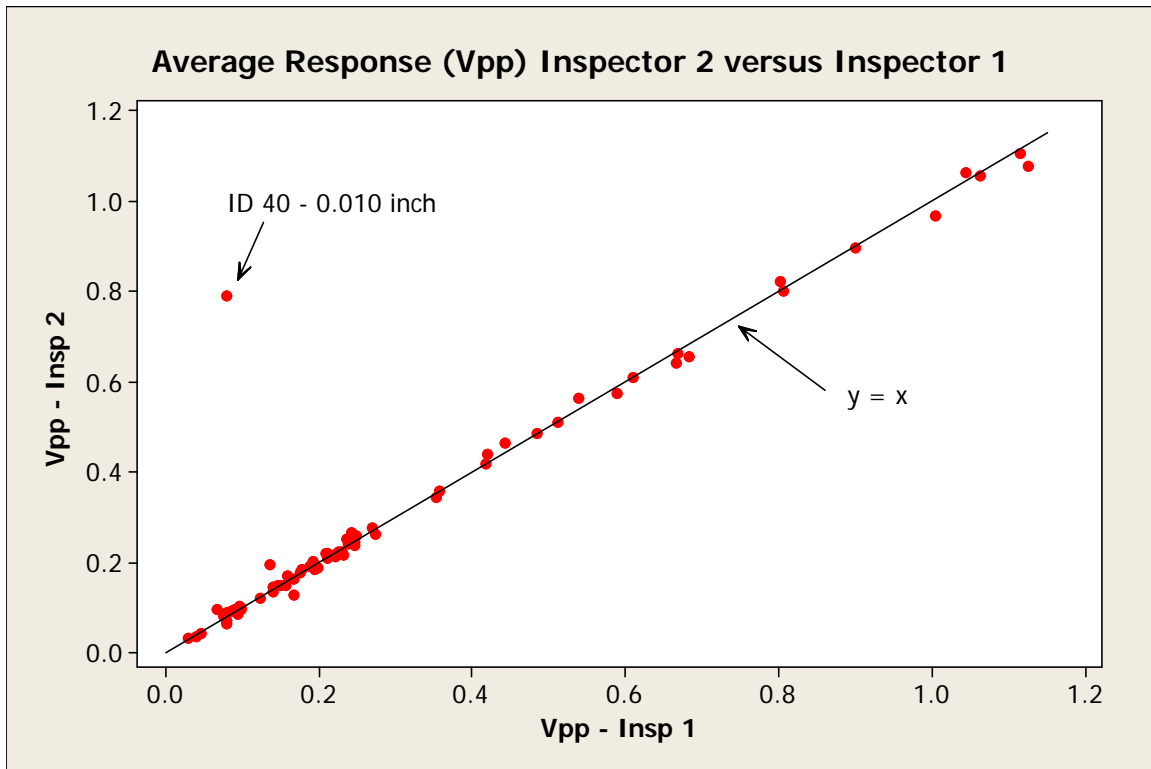
**Figure 5.5-7. Estimated POD Curves from Hit/Miss Data. 95 Percent Confidence on Crack Size yielding a POD of 0.90 is shown for Inspector 1**

A study with multiple cracks at inspection sites [ref. 1] reported that the analysis of hit/miss data using the largest crack size as the explanatory variable resulted in optimistic POD curves when applied to inspections of single cracks. Thus, the POD curve of Figure 5.5-7 applies to the detection of a cracked poppet simulator, characterized by the longest crack present, rather than the detection of a specific crack.

	<b>NASA Engineering and Safety Center Technical Assessment Report</b>	Document #: <b>NESC-RP-09-00506</b>	Version: <b>1.1</b>
Title: <b>STS-126 MPS#2 GH<sub>2</sub> Flow Control Valve Broken Poppet</b>		Page #: 42 of 59	

### 5.5.2 Signal Analysis

The initial analysis of the response signal data was to ascertain if the data exhibited an influence due to the individual inspector. The Vpp responses reported from individual poppet simulators by the two inspectors were compared, as shown in Figure 5.5-8, and nearly all of the measurements fall on a line with a slope of 1. The only exception was on poppet simulator #40, where the recorded Vpp value from Inspector 1 was an order of magnitude lower than that from Inspector 2. A re-examination of the recorded signals indicated that a clerical error had occurred and Inspector 2 had examined poppet simulator ID41 twice and had skipped poppet simulator ID40. Thus, only the one correct value for ID40 was carried through the analysis.



*Figure 5.5-8. The Vpp Response of Inspector 2 versus Inspector 1*

The inspectors recorded 6 inspections for each poppet simulator and the measurements from both inspectors were combined since no indication of systematic differences between inspectors was found. The standard deviation of the six Vpp measurements versus the average Vpp for each inspection indicates that the standard deviation increased as the mean response increased, as shown in Figure 5.5-9. This implies that uncertainty associated with the individual responses increased as the magnitude of the response increased. The ultimate goal was to perform a regression analysis for response as a function of crack size and to estimate the POD from the distributions derived from that analysis. Therefore, a transform of the response was considered to stabilize the uncertainty across the range of crack sizes. The log response was regressed



against the log crack size in an “a-hat” versus “a” analysis. However, the log response transformation overly compensates for a standard deviation that increases with increasing crack size and undercompensates for a standard deviation that decreases with increasing crack size. The family of power transforms (that includes the log transform as a special case) was chosen as candidates to stabilize the uncertainty across the crack size range.

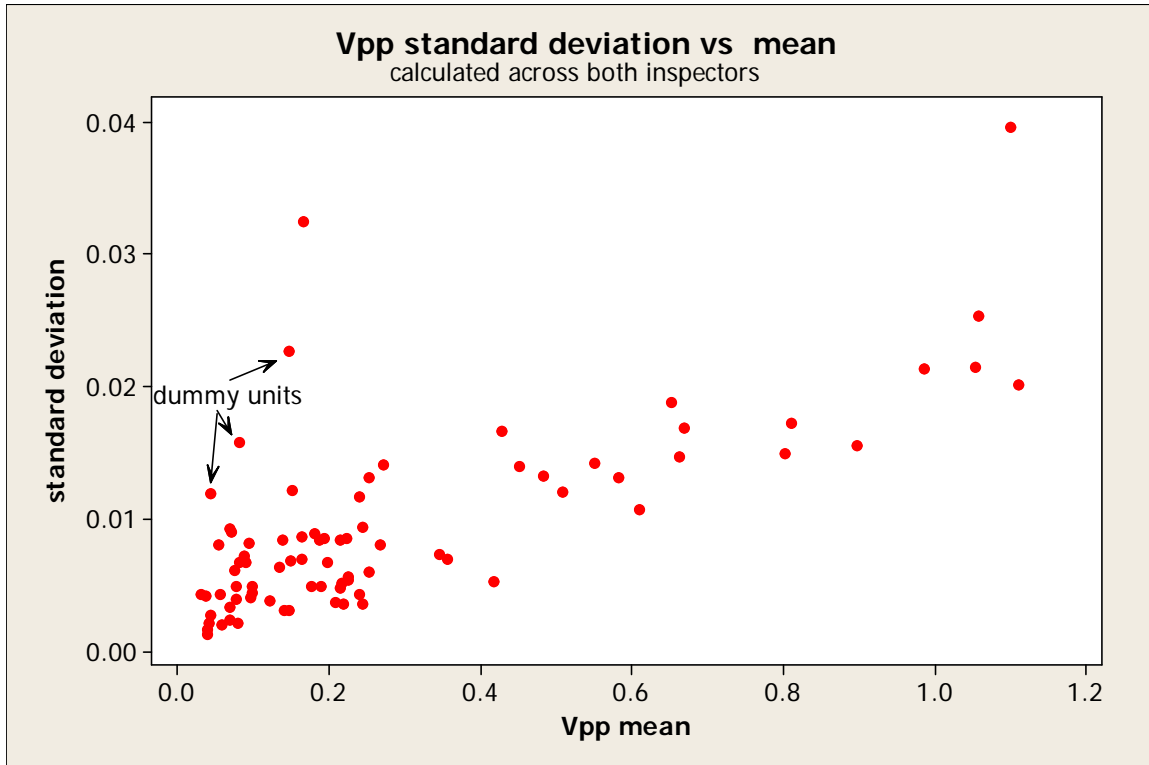


Figure 5.5-9. Standard Deviation versus Mean of the Vpp Responses (combined for both inspectors) for Individual Poppet Simulator Inspections

A power of 0.6 ( $x^{0.6}$ ) was found to provide the best stabilization of the variances for the entire crack size range, as shown in Figure 5.5-10. Note that, aside from a few extreme values, the tendency for standard deviation to increase with increasing crack sizes has been diminished. Three of the five points with largest standard deviations in Figure 5.5-10 were from inspections of the uncracked (control) poppet simulators. The remaining two points were from poppet simulators where the averages from the individual inspectors had the greatest difference. In other words, the higher standard deviations result from a combination of repeatability within inspector, and an inspector-to-inspector increase in variation.

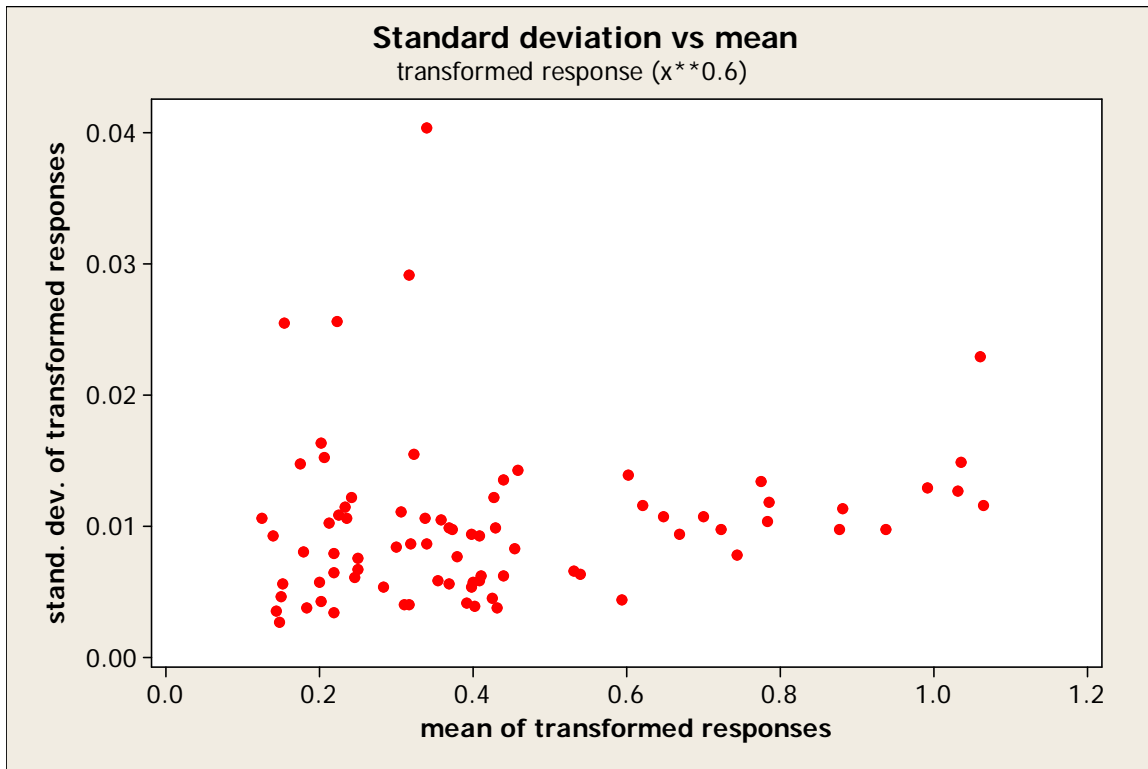


Figure 5.5-10. Standard Deviation versus Mean of the Vpp Responses Transformed by a Power of 0.6 (combined for both inspectors) for Individual Poppet Simulator Inspections

### 5.5.2.1 Longest Surface Crack Length as Explanatory Variable

The  $x^{0.6}$  transform on the Vpp responses were averaged and plotting against the longest crack length, as shown in Figure 5.5-11. The results were divided into 3 categories: no additional cracks; 1 or 2 additional cracks; and more than 3 additional cracks, according to how many cracks were located by the SEM examination of each loaded region. The number of cracks in a loading region did not appear to have a strong influence on the response level. Additional regression of the transformed response against both the “longest surface crack length” and “the number of additional cracks” confirmed this observation with statically significant ( $p < 0.001$ ) dependency on crack size and a statistically insignificant ( $p \sim 0.7$ ) dependency on the number of additional cracks.





Title:

STS-126 MPS#2 GH<sub>2</sub> Flow Control Valve Broken Poppet

Page #:

45 of 59

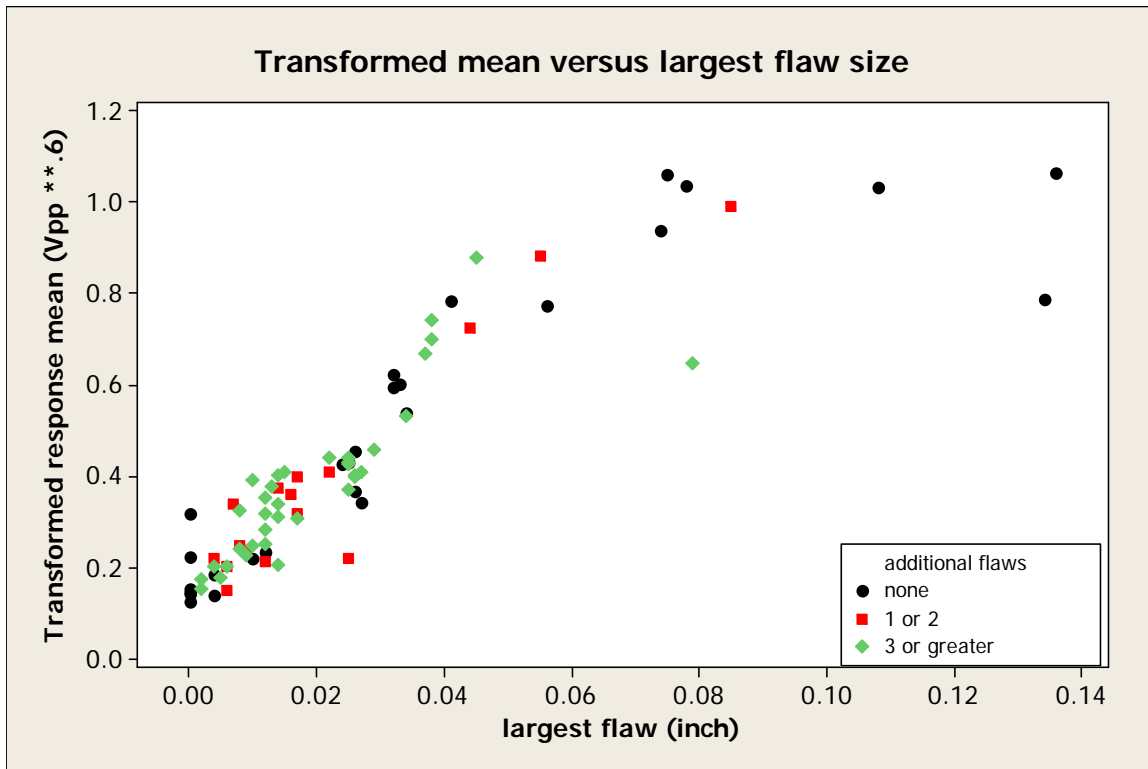



Figure 5.5-11. Transformed Response versus Largest Crack Length for Individual Poppet Simulator Inspections

A nearly linear relationship between the transformed response mean and the largest crack size appears to exist for crack lengths to approximately 0.06 to 0.08 inches (1.5 to 2.0 mm), as shown in Figure 5.5-11. The responses from the largest three cracks and a crack with a length of about 0.08 inches (2.0 mm) that had an atypically low transformed response were not included in the subsequent analysis to fit the linear region.

The poppet simulators had 19 loaded regions that were uncracked and four control poppet simulators. Both inspectors recorded Vpp measurements for all of the control poppet simulators and Inspector 1 recorded the response for one other loaded side where no cracks were located by the SEM examination. The responses in the uncracked loaded regions were modeled as censored observations, even though the inspectors did not record a response. Thus, the exact response value was unknown, but within a value in the interval of [0, C], where C had to be determined.

Examination of the inspection results revealed that the crack “hits” were not made solely on the magnitude of the Vpp response because some “hits” were reported with responses that were smaller than the responses of reported “misses”. The largest recorded transformed response that resulted in a “miss” call was 0.2490 (0.099 in the original scale) and the smallest recorded response that resulted in a “hit” call was 0.2115 (0.075 in the original scale). An approximate midpoint of this region of 0.225 (0.083 in original scale) was selected for the censoring level that was applied to the loaded regions where no cracks were found by the SEM evaluation and no

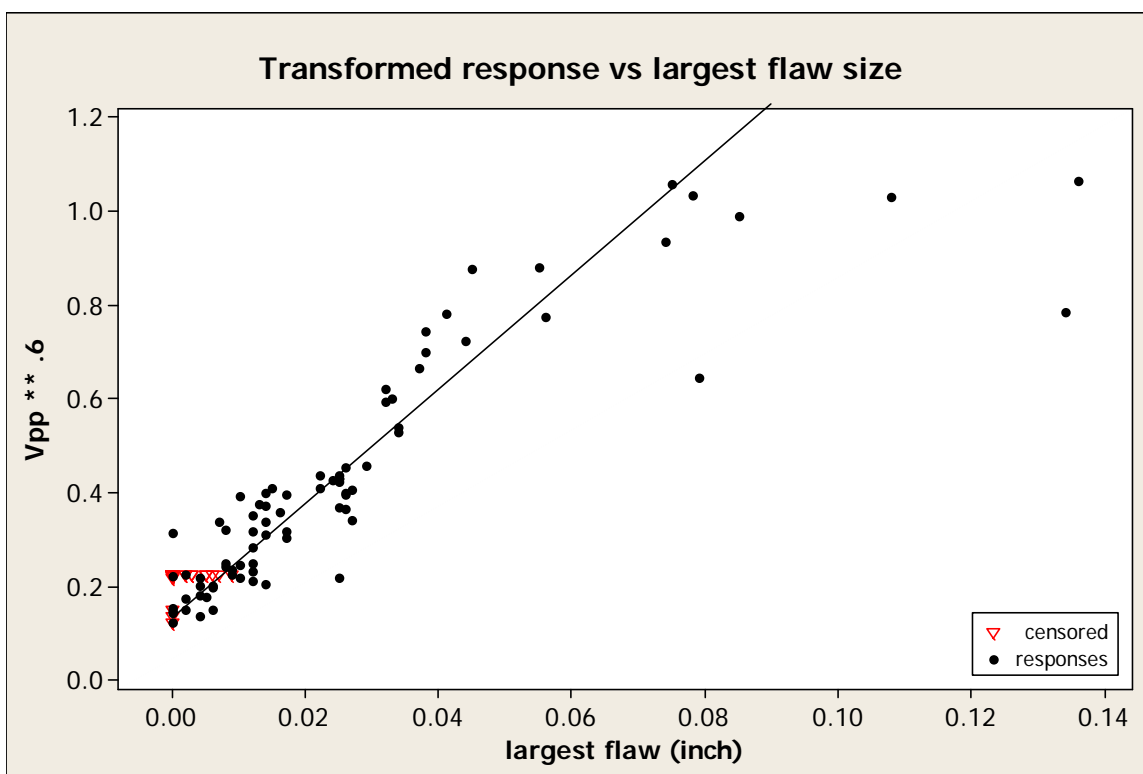
	<b>NASA Engineering and Safety Center Technical Assessment Report</b>	Document #: <b>NESC-RP- 09-00506</b>	Version: <b>1.1</b>
Title: <b>STS-126 MPS#2 GH<sub>2</sub> Flow Control Valve Broken Poppet</b>		Page #: 46 of 59	

inspection responses were recorded. The maximum likelihood estimates from this analysis yielded  $\hat{\mu} = 0.1304$ ,  $\hat{\sigma} = 0.0656$ . These values are not significantly different from the intercept and standard deviation estimated from the regression fit to the data that includes only the loaded regions with cracks. Thus, the crack data were combined with the no crack data and the resulting 106 data values (75 recorded plus 31 censored, but excluded the 4 long cracks noted earlier) were analyzed in a regression model.

A linear fit to this data yielded a mean regression line of:


$$V_{pp}^{.6} = 0.1353 + 12.1489 * \text{longest surface crack length.}$$

The variation of points around the mean characterized by a standard deviation estimate of  $\hat{\sigma} = 0.0711$ . This linear fit, overlaid with the observed and censored responses, is shown Figure 5.5-12.

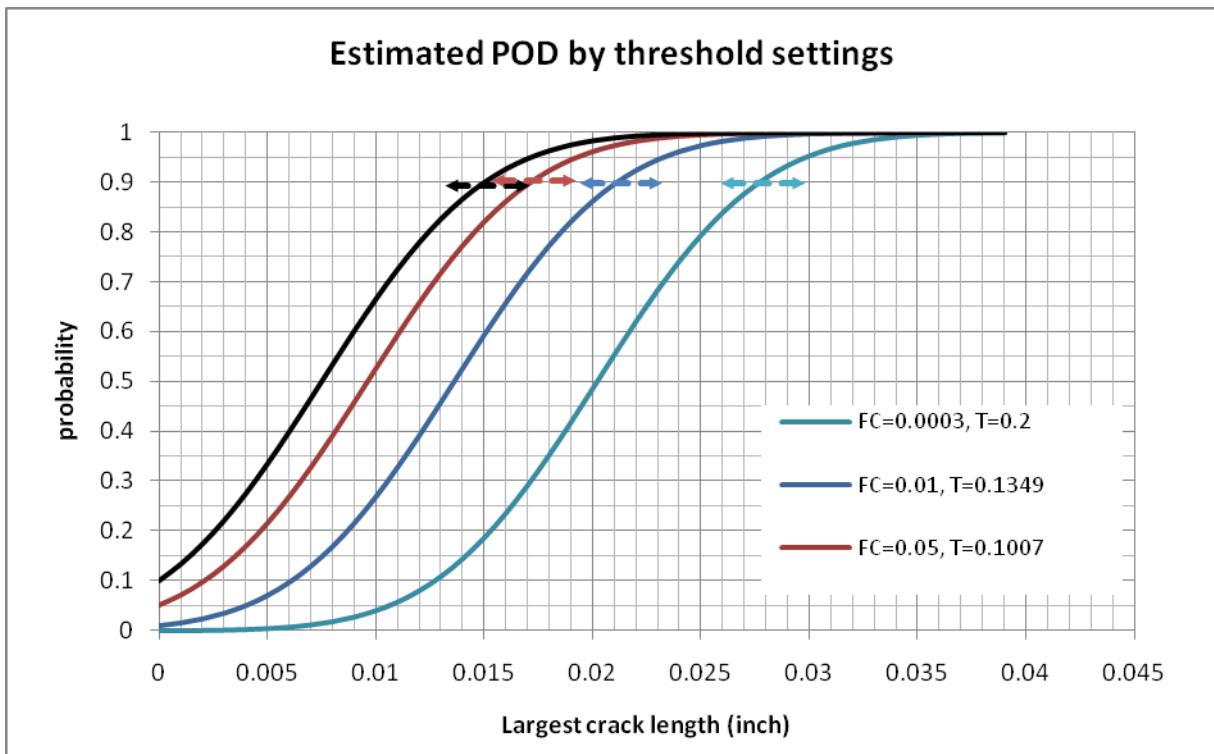


*Figure 5.5-12. Linear Fit in the Transform Scale with Censored Data Shown*

The POD curves derived from the fit parameters and different crack/no crack threshold values (T) are shown in Figure 5.5-13. Except for the threshold of 0.2 volt, the thresholds were the levels estimated to yield the corresponding false call rates. The 95 percent confidence interval for the crack length that has a 0.90 POD was determined using the likelihood ratio method and are shown by the arrows in Figure 5.5-13.

	<b>NASA Engineering and Safety Center Technical Assessment Report</b>	Document #: <b>NESC-RP- 09-00506</b>	Version: <b>1.1</b>
Title: <b>STS-126 MPS#2 GH<sub>2</sub> Flow Control Valve Broken Poppet</b>		Page #: 47 of 59	

The threshold level of 0.20 (probability) was included in Figure 5.5-13 because that level had been previously proposed for the screening of flight poppets. The estimated false call rate associated with the 0.20 threshold level was small (< 0.03 percent) based on the analysis that used the longest crack length as the explanatory variable.



**Figure 5.5-13. Estimated POD Curves from Signal Strength ( $V_{pp}$ ) versus size of Longest Crack. The 95 percent confidence on Crack Length Yielding a POD of 0.90 is shown for Threshold Level.**

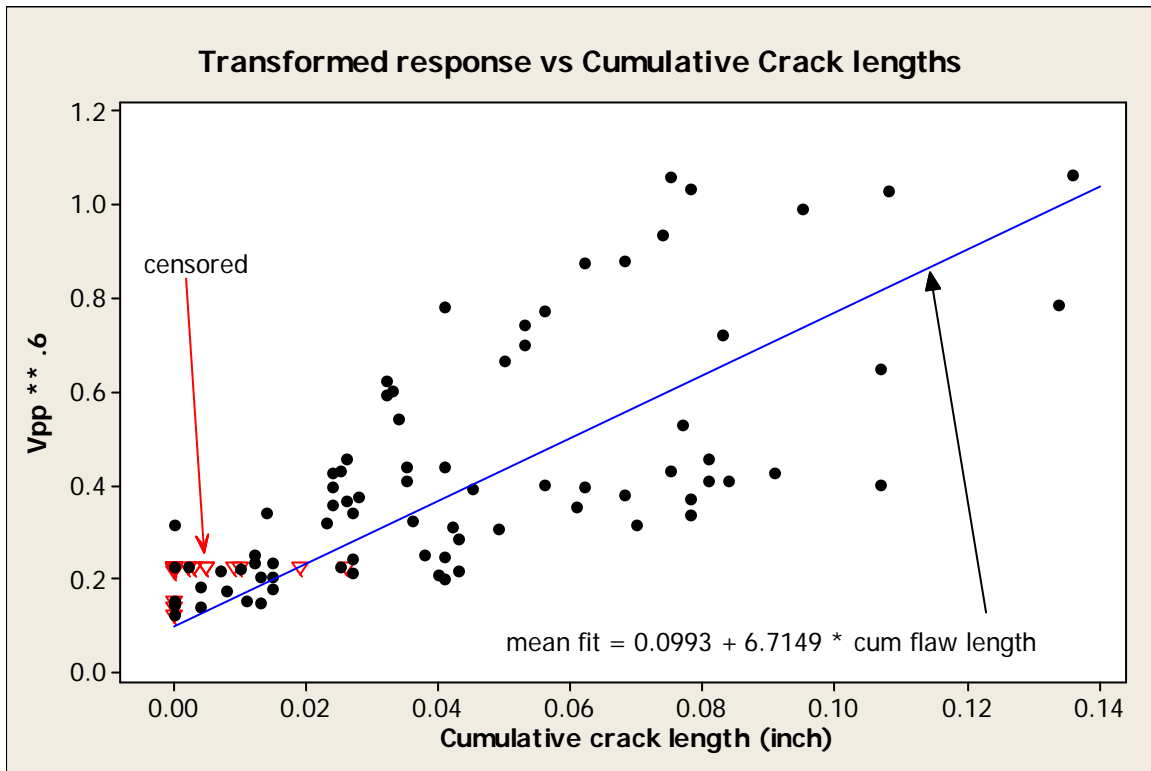
### 5.5.2.2 Cumulative Surface Crack Length as Explanatory Variable

The analysis presented in the previous section (signal regressed against the largest crack length) indicated a lack of dependence of the number of cracks present in the loaded regions on the  $V_{pp}$  response. However, an analysis that examined the cumulative damage of multiple cracks was evaluated because the structural integrity of an individual poppet and the probability of the poppet surviving a single flight may be influenced by the totality of damage. Thus, the regression analysis of the previous section was repeated using the cumulative lengths of all cracks in a loaded region as the explanatory variable. The linear fit to the transformed  $V_{pp}$  and cumulative crack length data resulted in the mean of regression line of:

$$V_{pp}^6 = 0.0993 + 6.7149 * \text{cumulative surface crack length.}$$

The variation of points around the mean was characterized by a standard deviation estimate of  $\hat{\sigma} = 0.1810$ , as shown in Figure 5.5-14. The results shown in Figure 5.5-14 indicated that the

variation about the mean line likely increased as the total crack lengths increased. However, as indicated with the response versus the longest crack length, it may be the case that the signal response would eventually flatten out. The data with respect to the cumulative crack length variable are not sufficient to estimate if and where this might occur.



*Figure 5.5-14. Transformed Response versus Cumulative Crack Lengths*

The POD curves were estimated for different threshold levels, as shown in Figure 5.5-15. The large variation around the mean line calculated using the cumulative crack length as the explanatory variable, resulted in the estimated false call rate for the proposed threshold level of 0.20 volts to be approximately 6 percent.

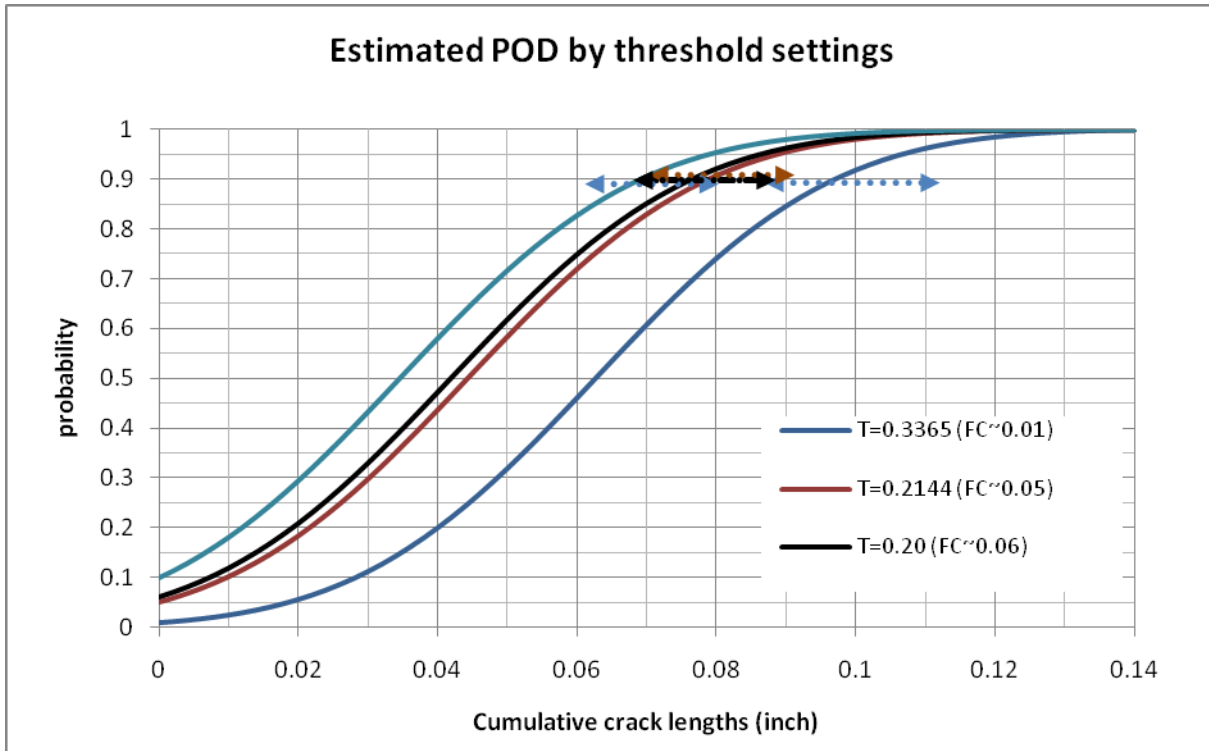


Figure 5.5-15. Estimated POD curves from signal strength ( $V_{pp}$ ) versus sum of all crack lengths in loaded region. The 95 percent confidence on crack length yielding a POD of 0.90 is shown for threshold level.

A comparison of the results calculated using the maximum crack length and the cumulative crack size as the explanatory variables indicated that the cumulative crack length was less effective in explaining the signal variations than was the maximum crack length. The finite dimensions of the probe and the nature of how the probe was swept in the radius suggested that the signal did not react equally to all the cracks in terms of surface length.

### 5.5.2.3 Cumulative Crack Area in Restricted Geography as Explanatory Variable

The accumulation of the cross sectional area of the cracks within a finite diameter circle was considered as an explanatory variable to evaluate the influence of multiple cracks on the  $V_{pp}$  response. The cross sectional area for each crack was estimated by assuming an elliptical shape and estimating the crack depth from the power law function of surface crack length previously given in Equation 1 and Figure 5.4-11. The largest accumulated crack area for a 0.040 inch (1.0 mm) diameter circle within the region-of-cracking was considered as the explanatory variable for signal strength, as shown in Figure 5.5-16.

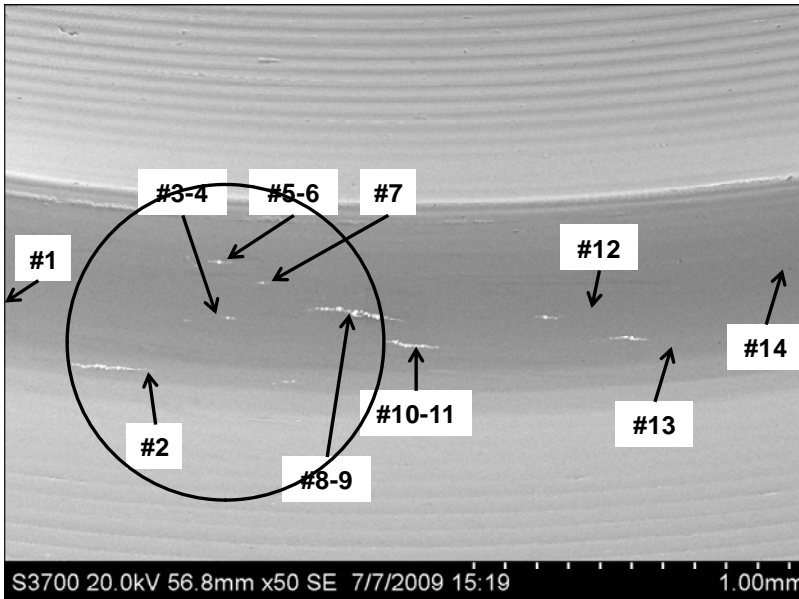


Title:

**STS-126 MPS#2 GH<sub>2</sub> Flow Control Valve Broken Poppet**

Page #:

50 of 59



Cracks 2, 3, 4, 5, 6, 7, 8, and 9 are within the 0.04" circle

$$\text{Aggregated Crack Length} = l_2 + l_3 + l_4 + l_5 + l_6 + l_7 + l_8 + l_9$$

$$m = 0.0823 \quad n = 0.7021 \text{ (see previous figure)}$$

$$\text{Aggregated Crack Area} = (1/4) * m * \pi (l_2^{n+1} + l_3^{n+1} + l_4^{n+1} + l_5^{n+1} + l_6^{n+1} + l_7^{n+1} + l_8^{n+1} + l_9^{n+1})$$

**Figure 5.5-16. Illustration of the Use of a 0.040 inch (1.0 mm) Circle for Accumulating Crack Area**

The accumulated area based on the observed surface crack lengths and the aspect ratio model described above was used as the explanatory variable and signal strength, as shown in Figure 5.5-17. The data had 12 instances where the surface crack length was more than 0.04 inches (1.0 mm) in length and for those 12 instances, the maximum crack length alone was used to determine the accumulated crack area. The data from Figure 5.5-17 were modified to use the area associated with a 0.04 inch (1.0 mm) crack for the 12 instances where the surface crack length exceeded this dimension, as shown in Figure 5.5-18. The linear fit to the transformed  $V_{pp}$  and accumulated area data resulted in the mean of regression line of:

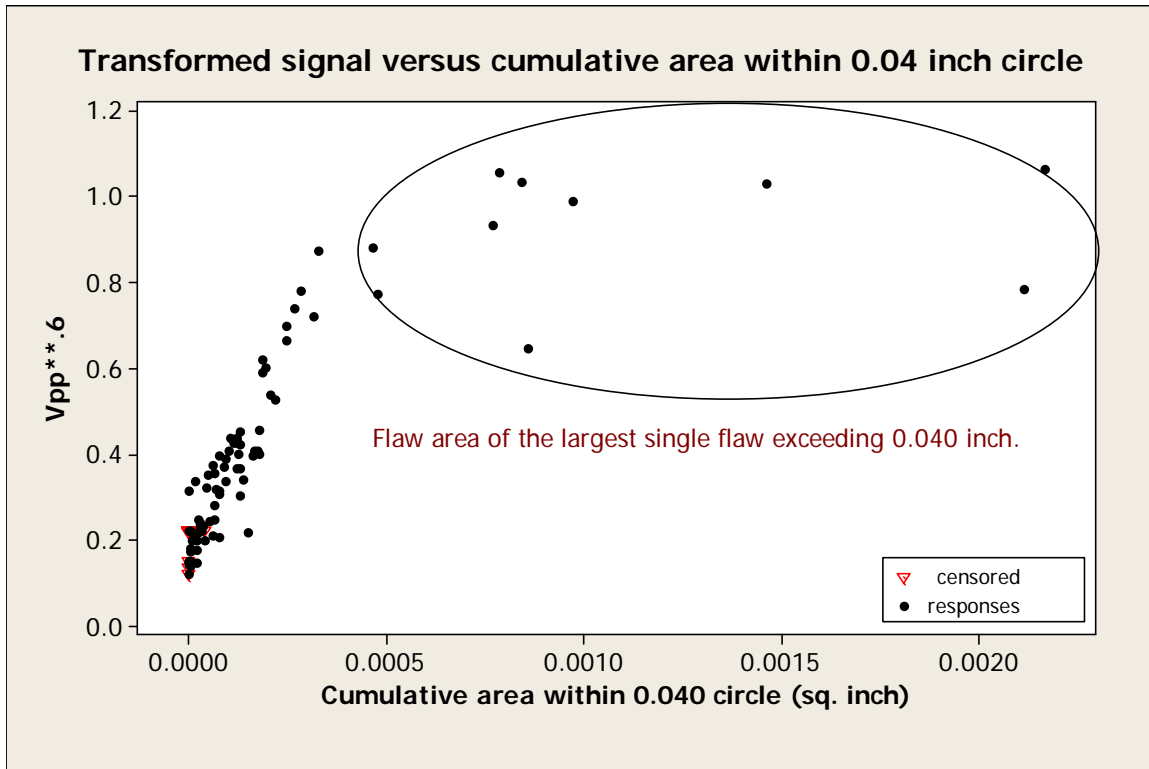
$$V_{pp}^6 = 0.1170 + 2512.7 * \text{cumulative crack area.}$$

The 10<sup>th</sup> percentile value was estimated based on the standard deviation estimate of  $\hat{\sigma} = 0.0917$ . The intersection of a threshold value for making a call with the 10<sup>th</sup> percentile line was at the  $a_{90}$  crack size. The horizontal line shown in Figure 5.5-18 corresponds to a threshold for  $V_{pp}$  of 0.2 ( $V_{pp}^6 = 0.3807$ ).

The POD curves were estimated using the above model and different threshold values, as shown in Figure 5.5-19. The false call rate was estimated for each of the threshold values. The value



associated with the nominal threshold of 0.20 volts was 0.2 percent, a value between the 0.03 percent for the largest crack length and the 6 percent for the cumulative crack length models.



*Figure 5.5-17. Transformed signal versus maximum cumulative area within 0.04 inch (1.0 mm) circle. Regions containing single cracks larger than 0.040 inch (1.0 mm) are shown with cross sectional area from the largest single crack.*

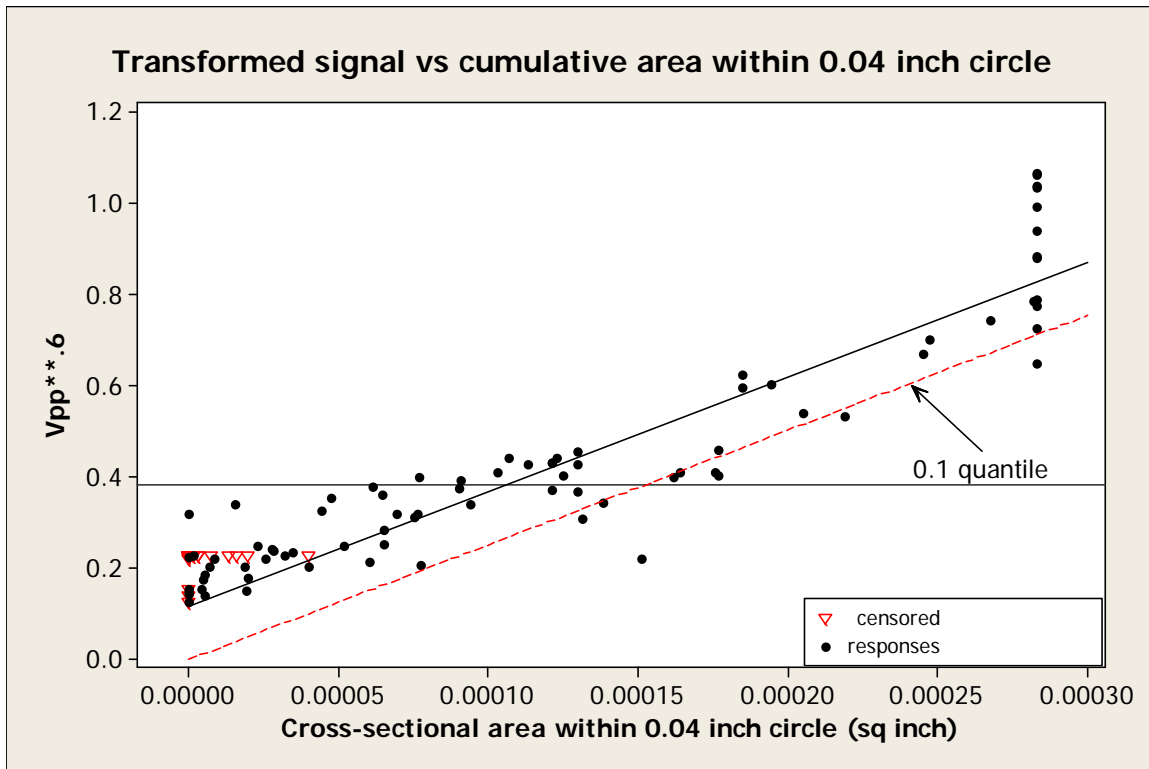


Figure 5.5-18. Transformed signal versus maximum cumulative area within 0.04 inch (1.0 mm) circle. Regions containing single cracks larger than 0.040 inch (1.0 mm) are shown with cross sectional area from the largest single crack.





Title:

STS-126 MPS#2 GH<sub>2</sub> Flow Control Valve Broken Poppet

Page #:

53 of 59

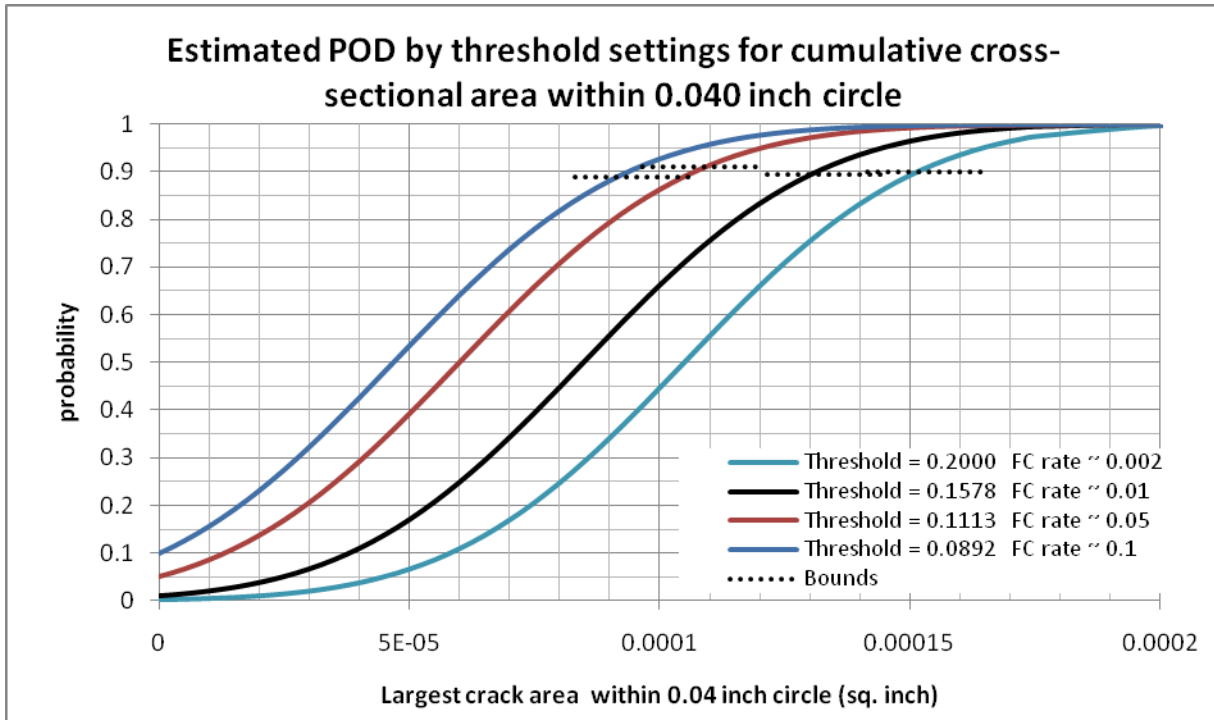


Figure 5.5-19. Estimated POD curves from signal strength ( $V_{pp}$ ) versus Cumulative Cross-Sectional area of Flaws within 0.04 inch (1.0 mm) Circle

## 6.0 Discussion of Summary Results

Poppet simulators were generated to reproduce the relevant material and geometric characteristics of the flight FCV poppet valves. Loading was applied to the flange of these simulators in two locations 180 degrees apart, resulting in a cyclic tensile stress in the area where cracks were observed in the flight FCV poppets. Although the actual loading was expected to result in fatigue cracks randomly distributed around the circumference of the flange, the simulators were loaded in a way to limit the area that would require detailed inspection by producing small fatigue cracks in known regions. A total of 72 poppet simulators were made for study, containing a total of 97 cracked regions. The largest individual crack for each cracked region was identified and found to range in size from 0.002 to 0.136 inches (0.05 to 3.5 mm). Of those cracks, 35 percent were 0.01 inches (0.25 mm) or less, 50 percent between 0.011 and 0.040 inches (0.28 to 1.0 mm), and the remaining 15 percent above 0.04 inches (1.0 mm).

Five of the poppet simulators were destructively examined, revealing the fracture surface of 16 cracks. The surface crack lengths obtained from the fracture surfaces correlated with those obtained from the SEM examination, indicating that this inspection method accurately identified the crack lengths to within 0.001 inches (0.03 mm). The destructive examination of the cracks also provided a measurement of the crack depth and shape that allowed the crack area to be estimated from the crack surface length in the intact poppet simulators. A catalog of the number



Title:

STS-126 MPS#2 GH<sub>2</sub> Flow Control Valve Broken Poppet

Page #:

54 of 59

of cracks, the surface crack lengths, the circumferential location of the cracks, and the results of the NDE inspections was developed, as shown in Appendix A.

Three regression models were used to derive POD curves, each having different explanatory variables to evaluate the influence of multiple cracks. The extent that any or all regression analyses reflect the actual probabilities associated with the EC inspection of flight poppets depends upon the fidelity of the simulated cracked poppets in representing the cracks that occur in service. Although the three regression models evaluated multiple cracks in a different manner, each can be thought of as being applied to a single surface crack measurement. However, this requires the translation of a cross sectional area back into a single surface crack length for the third model (cumulative cross-sectional area). This was performed by taking the POD curves derived for cross sectional area in Figure 5.5-19 and expressing the cross sectional area axis in the scale of a single surface crack length to yield the area, as shown in Figure 6.0-1 for the resultant POD curves.

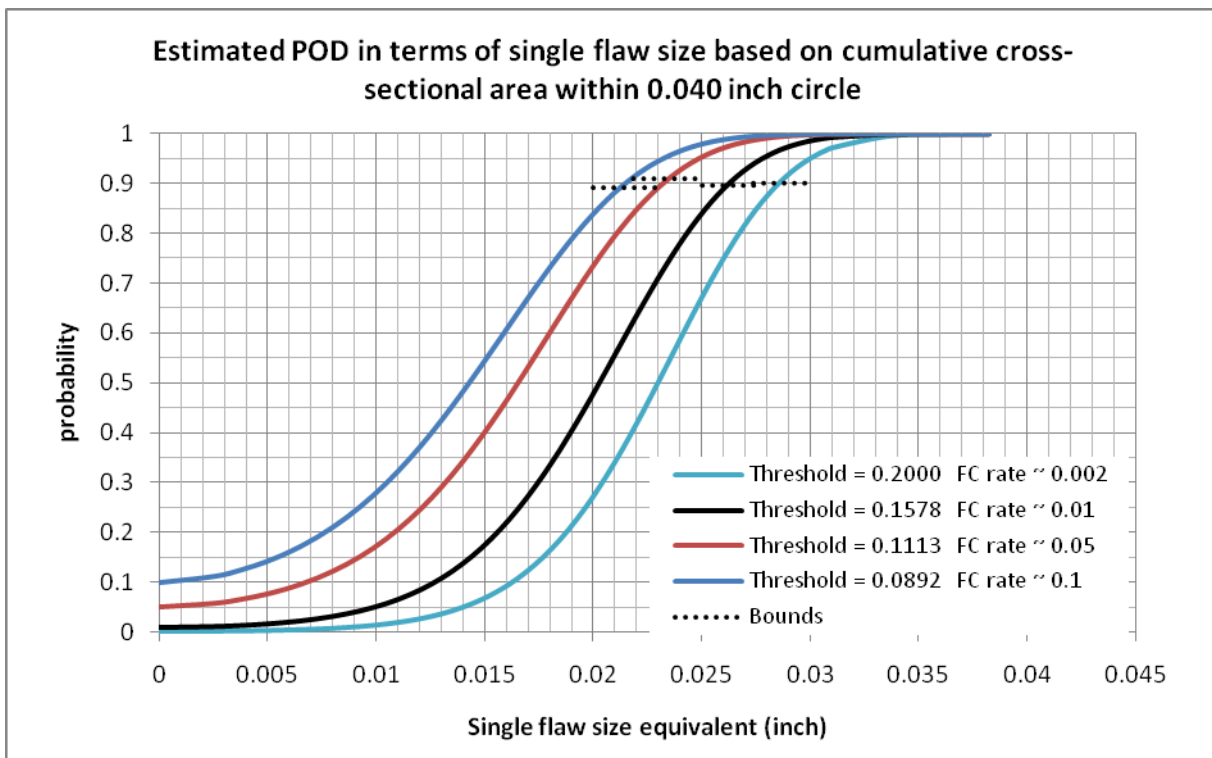



Figure 6.0-1. Estimated POD curves of Figure 5.5-19 with the x-axis transformed to the single surface crack length yielding the cross-sectional area estimates.

A comparison of Figures 5.5-19 and 5.5-13 shows a reasonably close agreement at the 0.2 Vpp threshold for the two POD curves. However, as the thresholds were relaxed (increasing the inspection sensitivity), there was not as much movement in the upper portion of the curves for those derived from the cumulative area model (Figure 5.5-19). The  $a_{90}$  estimated sizes tended to be larger for the models fit to the cumulative area data and the 95 percent confidence bounds

	<b>NASA Engineering and Safety Center Technical Assessment Report</b>	Document #: <b>NESC-RP- 09-00506</b>	Version: <b>1.1</b>
		Title: <b>STS-126 MPS#2 GH<sub>2</sub> Flow Control Valve Broken Poppet</b>	

tended to be somewhat tighter. Summary values for the  $a_{90}$  estimate and confidence bounds for all three models are contained in Table 6.0-1.

A measure of the “goodness of the fit” to the various regression models was provided by the standard deviation estimated for the residuals of the peak-to-peak voltages about the mean levels. The estimated standard deviations were: max crack-0.071; cumulative crack-0.181; cross-sectional area-0.092. The cumulative crack model provided the most conservative model, but was also the poorest fit. The maximum crack length model provided a better fit than the cross sectional area model, but it should be noted that the handling of the larger crack sizes in the two models was different. Some of the larger cracks were removed from the analysis with respect to the largest crack size as they were beyond where the linear assumption continued to hold. However, the larger cracks were retained in the cross sectional area analysis, but were limited to the maximum area used as a basis for the analysis.


**Table 6.0-1. Summary of  $a_{90}$  Estimates and Uncertainty**

	$a_{90}$ estimate	95 percent CI for $a_{90}$
Hit/miss Inspector 1	0.011	[0.009, 0.014]
Max flaw model (inch/mm)		
Thresh = 0.200, FC estimate =0.0003	0.028/0.71	[0.026, 0.030]
Thresh = 0.135, FC estimate =0.01	0.021/0.53	[0.019, 0.023]
Thresh = 0.101, FC estimate =0.05	0.017/0.43	[0.015, 0.019]
Thresh = 0.084, FC estimate =0.10	0.015/0.38	[0.013, 0.017]
Cumulative flaw lengths (inch/mm)		
Thresh = 0.337, FC estimate =0.01	0.097/2.46	[0.087, 0.112]
Thresh = 0.214, FC estimate =0.05	0.079/2.01	[0.070, 0.091]
Thresh = 0.200, FC estimate =0.06	0.076/1.93	[0.068, 0.088]
Thresh = 0.159, FC estimate =0.10	0.069/1.75	[0.061, 0.080]
Single flaw length corresponding to cross-sectional area model (inch/mm)		
Thresh = 0.200, FC estimate =0.002	0.029/0.74	[0.027, 0.030]
Thresh = 0.158, FC estimate =0.01	0.026/0.66	[0.025, 0.028]
Thresh = 0.111, FC estimate =0.05	0.023/0.58	[0.021, 0.025]
Thresh = 0.089, FC estimate =0.10	0.021/0.53	[0.020, 0.023]

## 7.0 Findings and NESC Recommendations

A POD study was conducted on cracked poppet simulators that replicated the behavior of flight MPS GH<sub>2</sub> FCV poppets. The critical characteristics of the FCV poppet were replicated in poppet simulators that were cracked using a specially designed loading fixture. The cracked poppet simulators were examined with a SEM to determine the length and location of all cracks greater than 0.001 inches (0.03 mm). A total of 55 cracked poppet simulators were created for the POD study with crack sizes that ranged from 0.001 to more than 0.1 inches (0.03 to 2.54 mm).

The measurements for the POD study were performed by two inspectors with identical EC systems with each inspector conducted six examinations of each poppet simulator. The results of

	<b>NASA Engineering and Safety Center Technical Assessment Report</b>	Document #: <b>NESC-RP- 09-00506</b>	Version: <b>1.1</b>
Title: <b>STS-126 MPS#2 GH<sub>2</sub> Flow Control Valve Broken Poppet</b>		Page #: 56 of 59	

the POD study recommend the continued used of a peak-to-peak output response voltage threshold of 0.2.

## 7.1 Findings


- F-1.** Two independent inspectors performed EC NDE inspections on 55 poppet simulators and detected all cracks that exceeded 0.01 inches (0.25 mm) in surface length.
- F-2.** A POD analysis was conducted that indicates the threshold of 0.2 volt for the signal strength that was initially recommended results in an inspection that is capable of finding cracks greater than 0.030 inches (0.76 mm) with probability exceeding 0.90. This capability has been established at a 95 percent confidence level. Estimated false call rates at this threshold level are small (< 0.002).
- F-3.** Cracks smaller than 0.030 inches (0.76 mm) are capable of being found by lowering the threshold from 0.2 volts, but with a tradeoff of increasing the false call rate.
- F-4.** The size and shape of the cracks that were detected in the poppet simulators were qualitatively similar in size and shape to the crack found in the failed flight poppet from STS-126.
- F-5.** The presence of multiple cracks in a small region had little or no influence on the EC findings.
- F-6.** The POD analysis found that the EC response was best characterized by the length of the largest crack in a region.

## 7.2 NESC Recommendations

- R-1.** The inspection of the SSP Orbiter MPS GH<sub>2</sub> FCV poppets should continue to use the 0.2 volt threshold as the accept/rejection criteria, as evaluated with the UniWest US 1779 bolt rotation device/scanner and a model US 1839 probe EC system, unless a critical crack size less than 0.030 inch (0.76 mm) is identified.<sup>1</sup> (**F-1, F-2, F-3, F-4, F-5, and F-6**)
  - a. If this crack length cannot be tolerated then the threshold will need to be re-examined and lowered to a level that balances the risks of passing a small crack with the estimated false call rate.
- R-2.** New inspectors<sup>2</sup> and/or EC inspections systems should be evaluating using the dataset of characterized cracked poppet simulators created during this study. (**F-1, F-2, F-3, F-4, F-5, and F-6**)

<sup>1</sup>Program has already moved to using a lowered detection threshold as well as assessing changes in signal response before and after testing or flight as part of the criteria to identify crack indications.

<sup>2</sup>NASA STD-5009 states that the period of certification for a special NDE procedure/inspector is 3 years. Thus, the inspectors would need to be re-certified within 3 years.

	<b>NASA Engineering and Safety Center Technical Assessment Report</b>	Document #: <b>NESC-RP- 09-00506</b>	Version: <b>1.1</b>
Title: <b>STS-126 MPS#2 GH<sub>2</sub> Flow Control Valve Broken Poppet</b>		Page #: 57 of 59	

## 8.0 Alternate Viewpoints

There were no alternate viewpoints during the course of this assessment.

## 9.0 Other Deliverables

There are no other deliverables after the final report is completed and approved by the NRB.

## 10.0 Lessons Learned

No applicable lessons learned were identified for entry into the NASA Lessons Learned Information System (LLIS).

## 11.0 Definition of Terms

### Corrective Actions

Changes to design processes, work instructions, workmanship practices, training, inspections, tests, procedures, specifications, drawings, tools, equipment, facilities, resources, or material that result in preventing, minimizing, or limiting the potential for recurrence of a problem.

### Finding

A conclusion based on facts established during the assessment/inspection by the investigating authority.

### Lessons Learned

Knowledge or understanding gained by experience. The experience may be positive, as in a successful test or mission, or negative, as in a mishap or failure. A lesson must be significant in that it has real or assumed impact on operations; valid in that it is factually and technically correct; and applicable in that it identifies a specific design, process, or decision that reduces or limits the potential for failures and mishaps, or reinforces a positive result.

### Observation


A significant factor established during this assessment that supports and influences the conclusions reached in the statement of Findings and Recommendations.

### Off-Nominal Surface

Off-nominal surface is defined as a surface finish that does not meet specification/drawing requirements.

### Problem

The subject of the independent technical assessment/inspection.

	<b>NASA Engineering and Safety Center Technical Assessment Report</b>	Document #: <b>NESC-RP- 09-00506</b>	Version: <b>1.1</b>
Title: <b>STS-126 MPS#2 GH<sub>2</sub> Flow Control Valve Broken Poppet</b>		Page #: 58 of 59	

### Recommendation

An action identified by the assessment/inspection team to correct a root cause or deficiency identified during the investigation. The recommendations may be used by the responsible C/P/P/O in the preparation of a corrective action plan.

### Repliset


A tough, flexible mold material that is used to obtain high-resolution replicas of engineering surfaces for microscopic surface examinations.

### Root Cause

Along a chain of events leading to a mishap or close call, the first causal action or failure to act that could have been controlled systemically either by policy/practice/procedure or individual adherence to policy/practice/procedure.

## 12.0 Acronyms List

AS&M	Analytical Systems and Materials, Inc.
CFD	Computational Fluid Dynamics
EC	Eddy Current
EDM	Electro-Discharge Machining
ET	External Tank
FCV	Flow Control Valve
GH <sub>2</sub>	Gaseous Hydrogen
H <sub>RC</sub>	Hardness Rockwell C
IACS	International Annealed Copper Standard
JSC	Johnson Space Center
LaRC	Langley Research Center
LV	Launch Vehicle
LH <sub>2</sub>	Liquid Hydrogen
MPS	Main Propulsion System
MTSO	Management and Technical Support Office
NASA	National Aeronautics and Space Administration
NDE	Nondestructive Evaluation
NESC	NASA Engineering and Safety Center
NRB	NESC Review Board
OV	Orbiter Vehicle
POD	Probability of Detection
rpm	Revolutions per Minute
SEM	Scanning Electron Microscope
SEO	Systems Engineering Office
SSME	Space Shuttle Main Engine
SSP	Space Shuttle Program

	<b>NASA Engineering and Safety Center Technical Assessment Report</b>	Document #: <b>NESC-RP- 09-00506</b>	Version: <b>1.1</b>
Title: <b>STS-126 MPS#2 GH<sub>2</sub> Flow Control Valve Broken Poppet</b>		Page #: 59 of 59	

STS           Space Transportation System  
 TDT           Technical Discipline Team  
 Vpp           Volts – peak to peak

## 13.0 References

1. "Probability of Detection Estimation fro Hit/Miss Data When Detection Cannot be Attributed to Specific Flaws: An Explanatory Data Analysis," Spencer, Floyd, in Review of Progress in Quantitative Nondestructive Evaluation, Vol. 25, edited by D.O. Thompson and D.E. Chimenti, American Institute of Physics, 2006.

## Volume II- Appendices (stand-alone volume)

- A. Poppet Simulator Data
- B. Boeing Eddy Current Procedure/Technique Sheet Flow Control Valve Poppet - #SSO-01, Revision C

**REPORT DOCUMENTATION PAGE**

*Form Approved  
OMB No. 0704-0188*

The public reporting burden for this collection of information is estimated to average 1 hour per response, including the time for reviewing instructions, searching existing data sources, gathering and maintaining the data needed, and completing and reviewing the collection of information. Send comments regarding this burden estimate or any other aspect of this collection of information, including suggestions for reducing this burden, to Department of Defense, Washington Headquarters Services, Directorate for Information Operations and Reports (0704-0188), 1215 Jefferson Davis Highway, Suite 1204, Arlington, VA 22202-4302. Respondents should be aware that notwithstanding any other provision of law, no person shall be subject to any penalty for failing to comply with a collection of information if it does not display a currently valid OMB control number.  
**PLEASE DO NOT RETURN YOUR FORM TO THE ABOVE ADDRESS.**

<b>1. REPORT DATE (DD-MM-YYYY)</b> 01-03-2011		<b>2. REPORT TYPE</b> Technical Memorandum		<b>3. DATES COVERED (From - To)</b> February 2009 - March 2011	
<b>4. TITLE AND SUBTITLE</b> Space Shuttle Program (SSP) Orbiter Main Propulsion System (MPS) Gaseous Hydrogen (GH2) Flow Control Valve (FCV) Poppet Eddy Current (EC) Inspection Probability of Detection (POD) Study				<b>5a. CONTRACT NUMBER</b>	
				<b>5b. GRANT NUMBER</b>	
				<b>5c. PROGRAM ELEMENT NUMBER</b>	
<b>6. AUTHOR(S)</b> Piascik, Robert S.; Prosser, William H.				<b>5d. PROJECT NUMBER</b>	
				<b>5e. TASK NUMBER</b>	
				<b>5f. WORK UNIT NUMBER</b> 869021.03.07.01.07	
<b>7. PERFORMING ORGANIZATION NAME(S) AND ADDRESS(ES)</b> NASA Langley Research Center Hampton, VA 23681-2199				<b>8. PERFORMING ORGANIZATION REPORT NUMBER</b>  L-20006 NESC-RP-09-00506	
<b>9. SPONSORING/MONITORING AGENCY NAME(S) AND ADDRESS(ES)</b> National Aeronautics and Space Administration Washington, DC 20546-0001				<b>10. SPONSOR/MONITOR'S ACRONYM(S)</b>  NASA	
				<b>11. SPONSOR/MONITOR'S REPORT NUMBER(S)</b> NASA/TM-2011-217072/Volume I	
<b>12. DISTRIBUTION/AVAILABILITY STATEMENT</b> Unclassified - Unlimited Subject Category 16 - Space Transportation and Safety Availability: NASA CASI (443) 757-5802					
<b>13. SUPPLEMENTARY NOTES</b>					
<b>14. ABSTRACT</b> The Director of the NASA Engineering and Safety Center (NESC), requested an independent assessment of the anomalous gaseous hydrogen (GH2) flow incident on the Space Shuttle Program (SSP) Orbiter Vehicle (OV)-105 during the Space Transportation System (STS)-126 mission. The main propulsion system (MPS) engine #2 GH2 flow control valve (FCV) LV-57 transition from low towards high flow position without being commanded. Post-flight examination revealed that the FCV LV-57 poppet had experienced a fatigue failure that liberated a section of the poppet flange. The NESC assessment provided a peer review of the computational fluid dynamics (CFD), stress analysis, and impact testing. A probability of detection (POD) study was requested by the SSP Orbiter Project for the eddy current (EC) nondestructive evaluation (NDE) techniques that were developed to inspect the flight FCV poppets. This report contains the findings and recommendations from the NESC assessment.					
<b>15. SUBJECT TERMS</b> Computational fluid dynamics; Nondestructive evaluation; NASA Engineering and Safety Center; Flow control valve; Anomalous gaseous hydrogen flow; Poppet					
<b>16. SECURITY CLASSIFICATION OF:</b>			<b>17. LIMITATION OF ABSTRACT</b>	<b>18. NUMBER OF PAGES</b>	<b>19a. NAME OF RESPONSIBLE PERSON</b>
<b>a. REPORT</b>	<b>b. ABSTRACT</b>	<b>c. THIS PAGE</b>			STI Help Desk (email: help@sti.nasa.gov)
U	U	U	UU	64	<b>19b. TELEPHONE NUMBER (Include area code)</b> (443) 757-5802